



Chem Soc Rev

Polycatenanes: synthesis, characterization, and physical understanding

Journal:	<i>Chemical Society Reviews</i>
Manuscript ID	CS-REV-04-2022-000256.R1
Article Type:	Review Article
Date Submitted by the Author:	16-May-2022
Complete List of Authors:	Liu, Guancen; University of Chicago Division of the Physical Sciences, Department of Chemistry Rauscher, Phillip; University of Chicago Division of the Physical Sciences, Pritzker School of Molecular Engineering Rawe, Benjamin; University of Chicago Division of the Physical Sciences, Pritzker School of Molecular Engineering Tranquilli, Marissa M; University of Chicago Division of the Physical Sciences, Pritzker School of Molecular Engineering Rowan, Stuart; University of Chicago Division of the Physical Sciences, Pritzker School of Molecular Engineering; University of Chicago Division of the Physical Sciences, Department of Chemistry

SCHOLARONE™
Manuscripts

ARTICLE

Polycatenanes: synthesis, characterization, and physical understanding†

Received 00th January 20xx,
Accepted 00th January 20xx

Guancen Liu,^a Phillip M. Rauscher,^b Benjamin W. Rawe,^b Marissa M. Tranquilli,^a and Stuart J. Rowan^{*abc}

DOI: 10.1039/x0xx00000x

Chemical composition and architecture are two key factors that control the physical and material properties of polymers. One of the more unusual and intriguing polymer architectures are the polycatenanes, which are a class of polymers that contain mechanically interlocked rings. Since the development of high yielding synthetic routes to catenanes, there has been an interest in accessing their polymeric counterparts, primarily on account of the unique conformations and degrees of freedom offered by non-bonded interlocked rings. This has led to the synthesis of a wide variety of polycatenane architectures and to studies aimed at developing structure-property relationships of these interesting materials. In this review, we provide an overview of the field of polycatenanes, exploring synthesis, architecture, properties, simulation, and modelling, with a specific focus on some of the more recent developments.

Introduction

Across the family of mechanically interlocked molecules, there are many structures that offer intriguing opportunities to access polymeric materials that exhibit new or unusual properties.^{1–5} The non-covalent and potentially highly mobile nature of the interlocking components presents a framework for accessing unique dynamic and rheological properties⁶ when integrated into polymeric architectures. Of the different interlocking motifs, one class that has attracted attention^{7–11} in the field of polymer science is the catenane, which consists of two or more interlocked rings. Perhaps one of the attractions of materials composed of interlocked rings is the fact that there are many instances where such structures have been utilized in macroscopic materials, such as chain-links and chainmail. These macroscopic materials derive their combination of flexibility and strength from the mobility of the individual rings within the structure. Translating these macroscopic structures to the molecular level has the potential to allow access to materials with new property profiles,^{12,13} as the mechanical bond that holds the rings together allows them to rotate, elongate/collapse, and twist relative to their interlocked partner (Fig. 1a).

A primary challenge to the widespread study and application of polycatenane-based materials is their synthesis. At some point in their synthesis, the formation of one or more macrocycles is required; unfortunately, such reactions are not

usually high yielding.¹⁴ None-the-less, researchers have developed synthetic routes to a wide-variety of polycatenane structures.⁹ For example, one approach is to synthesize small molecule catenanes and (co)polymerize them into linear or network polymeric materials. In fact, some of the earliest examples of polycatenanes are the poly[2]catenanes that were prepared by the polymerization of a monomeric [2]catenane (the two refers to the number of rings in the catenane).¹⁵ Depending on the specific placement of the polymerizable groups, the polymerization can yield a main-chain poly[2]catenane (Fig. 1b) in which the catenane is part of the polymer backbone or side-chain/“pendant” poly[2]catenanes, where the catenane is attached off of the polymer backbone (Fig. 1c).¹⁶

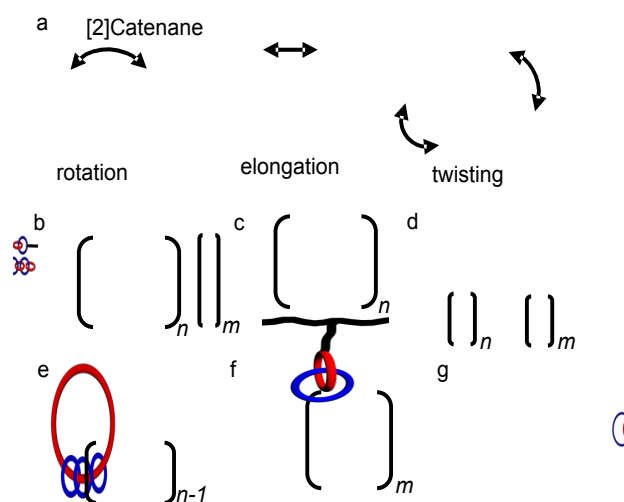


Fig. 1 Schematic representation of (a) the motions of the components within a [2]catenane, (b) a main-chain poly[2]catenane, (c) side-chain/pendant poly[2]catenane, (d) a polymeric [2]catenane, (e) a polymeric radial [n]catenane, (f) a linear poly[n]catenane and (g) a poly[n]catenane network/Olympic gel. Reproduced from Ref. 7 with permission from Springer Nature.

^a Department of Chemistry, University of Chicago, Chicago, IL, USA.

^b Pritzker School of Molecular Engineering, University of Chicago, Chicago, IL, USA

^c Chemical and Engineering Sciences, Argonne National Laboratory, Lemont, IL, USA

† The review is dedicated to one of the true pioneers of the catenane field Sir Fraser Stoddart on occasion of his 80th birthday.

A different class of polycatenanes consists of two interlocked large ring polymers to create a polymeric [2]catenane (Fig. 1d). This is an interesting architecture as it can be thought of as two permanently entangled polymers and, as such, offers a model for studying the physical principles of polymer entanglements.^{17,18}

Polymers can also be accessed in which the entire architecture is composed of only interlocking rings (Fig. 1e-g). In such poly[*n*]catenanes, the density of the mechanical bond present in the structure is optimized, maximizing their effect on the material properties. An example of this optimization can be found in the polymeric radial [*n*]catenane (Fig. 1e), constructed by threading a single large polymeric macrocycle with *n*-1 smaller macrocycles.¹⁹⁻²¹ This structure is able to demonstrate

a molecular motion not present in any of the previously mentioned polycatenanes, namely, the sliding of the small ring around the large ring, reminiscent of the translational molecular motions possible in a different type of mechanically interlocked polymer, the main-chain polyrotaxanes.^{4,22,23} Another entirely catenated polymer is classified as the linear poly[*n*]catenane (Fig. 1f),¹³ a structure in which each macrocyclic subunit is interlocked with two other rings. Finally, branched poly[*n*]catenanes are also possible if a few of these macrocycles are interlocked with more than two rings. Increasing the density of macrocycles interlocked with three or more rings leads to poly[*n*]catenane networks or Olympic gels (Fig. 1g).

No matter the structure of the polycatenane there are two main synthetic requirements: formation of the catenane and

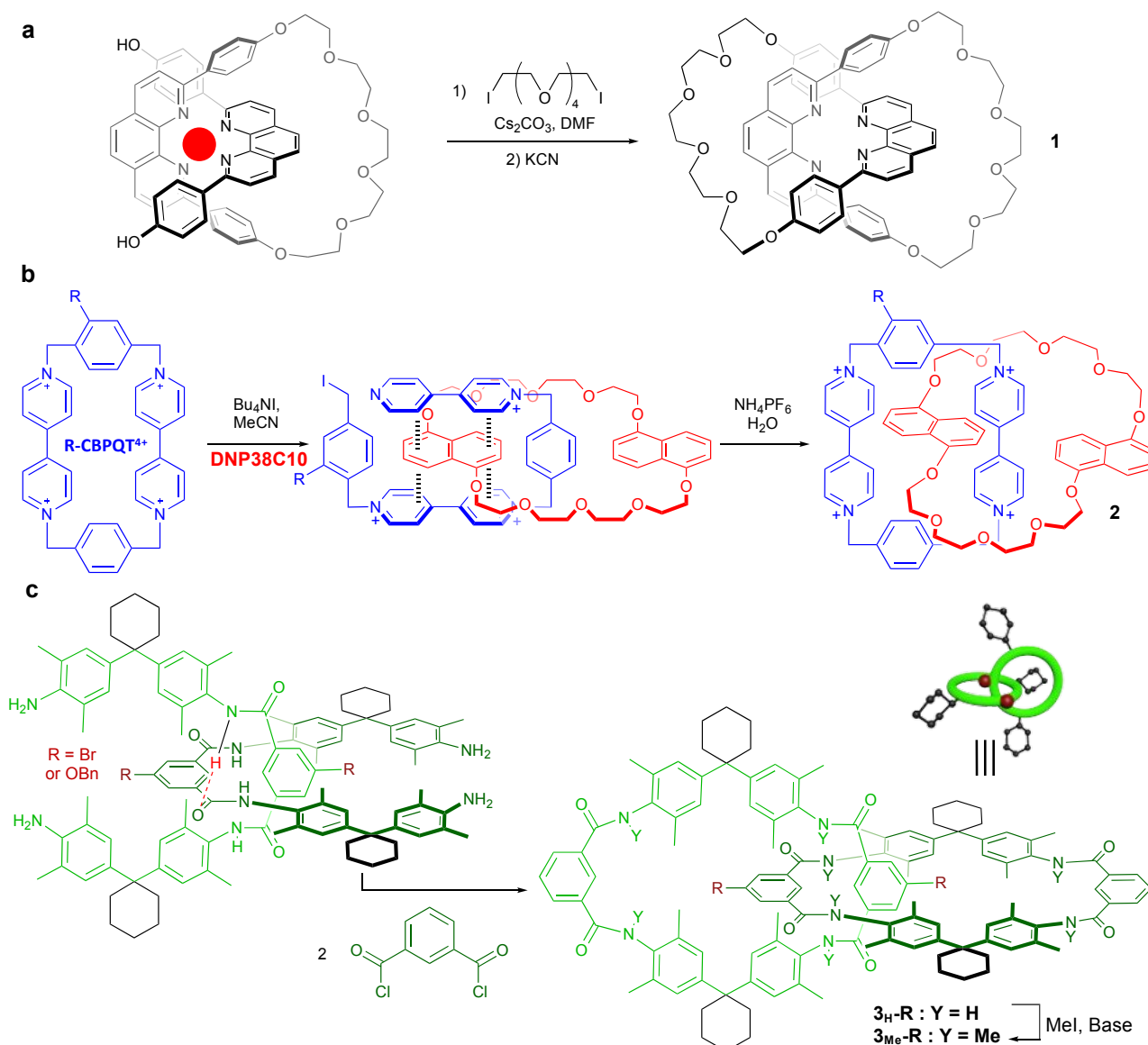


Fig. 2 a) An example of transition metal ion templating to create a [2]catenane (**1**) using Cu^+ ion (red) templating. b) The use of π - π stacking between an electron poor tetracationic cyclophane (blue, **CBPQT⁴⁺**) and an electron rich naphthalene-based crown ether (red, **DNP38C10**) to template the synthesis of **2**. c) Amide hydrogen bonding (highlighted in red) is used to access the [2]catenane **3**, and a schematic representation of **3** where the position of the functional groups (R, burgundy) and cyclohexane moieties (black) are indicated. Bn = CH_2Ph

polymerization, although not necessarily in that order. As such, it is important to understand the principles of these two reactions and how they complement or compete with each other.

Of course, the chemistry of polycatenanes is only half the story. Indeed, as with any polymer, the resulting physical and material properties will ultimately dictate any technological application. Thus, it is crucial for researchers to combine new polycatenane syntheses with established concepts in polymer physics and engineering to develop a more complete understanding of these systems. This part of the field has blossomed in recent years, particularly on account of an influx of new computational studies, which can more directly answer questions concerning the nature and effects of mechanical bonds on polymer and material properties. While many questions remain unanswered, a significant corpus of knowledge has begun to crystallize, so that some key insights can now be gleaned.

The goal of this review article is to discuss in a pedagogical manner both sides of the polycatenane story described above: chemical synthesis and physical understanding. We begin by discussing the former in a slightly different manner than in previous reviews on the topic. Rather than focusing on each of the various polycatenane architectures (Fig. 1) individually, we instead take a methodological viewpoint grounded in the two key aspects of polycatenane synthesis introduced above: catenation and polymerization. We first summarize popular methods for synthesizing small molecule catenanes and then show how these methods may be combined with polymerization strategies to prepare macromolecular species. We then discuss the emerging physical understanding of polycatenanes through the lenses of three foundational concepts in polymer physics: molecule size and scaling, elasticity, and dynamics and rheology. We then offer some brief remarks on future directions for the field.

Common methods for small molecule catenane synthesis

Though the first synthetic catenanes reported were formed via statistical assembly,²⁴ most catenane syntheses nowadays utilize a templated approach to ensure that the individual components are appropriately positioned for catenation.^{8,25} One way to achieve such templating is to design non-covalent interactions into the starting compounds such that they self-assemble in a manner that facilitates catenane formation upon ring closure. A wide range of supramolecular motifs have been exploited to achieve this, including but not limited to metal ion–ligand coordination,^{26,27} π – π stacking or aromatic donor–acceptor interactions,^{28–30} hydrogen bonding,³¹ as well as combinations of these non-covalent interactions.²⁵

For catenane synthesis that relies on metal ion–ligand coordination, commonly referred to as (passive) transition-metal (TM) templating, the assembly relies on the defined nature of the metal ion coordination geometry. This method requires starting materials with ligand components that

coordinate and organize around the TM template such that, when the macrocycles are formed, the result (Fig. 2a) is a catenate (metalated catenane). TM templating is appealing as the noncovalent interactions that drive the assembly can be easily removed after the catenation step: washing the catenate with a stronger ligand can remove the metal ion and result in a catenane, which has been termed, in some literature, a catenand on account of the fact that these catenanes contain ligands (Fig. 2a).²⁶ TM templated catenane synthesis was pioneered by Sauvage in 1983 when he used a Cu⁺:phenanthroline complex to synthesize catenane **1**.³² Since that initial work, other transition metal ions, including Fe²⁺, Zn²⁺, and Pd²⁺, and ligands have been employed in the efficient synthesis of catenanes.^{8,33–36}

The use of π – π /aromatic donor–acceptor interactions have been extensively employed to access interlocked molecules. One of the more utilized approaches is the incorporation of electron-poor aromatic units into one component with the second component containing π -electron rich aromatic units. This approach was pioneered and employed heavily by Stoddart and coworkers,³⁷ who have shown that it is possible to synthesise catenanes using such supramolecular motifs by either kinetic or thermodynamic control.³⁸ Fig. 2b shows an example of the thermodynamic-controlled synthesis, in which the resulting catenane **2** consists of the π -electron-accepting macrocycle, cyclobis(paraquat-*p*-phenylene) (**R-CBPQT⁴⁺**) interlocked with the electron rich crown ether (**DNP38C10**).³⁹

Hydrogen-bond driven assembly is another common approach used in catenane synthesis. Fig. 2c shows an example of this that relies on amide functionalities to self-assemble the components into the appropriate configuration.^{40,41} Ring closing of such template assemblies can yield [2]catenanes, such as the amide-containing **3**.^{42–47}

Methods utilized for the synthesis of polycatenanes

In addition to making the catenane, a polymerization step is required to synthesize a polycatenane. Conceptually, the polymerization process can take place before, after, or even during the synthesis of the catenane. The specific ordering of these steps is dependent on the polycatenane architecture that is being targeted and the compatibility of the functionalities that are used in the catenation/polymerization steps. This mix of molecular and polymer chemistry stratagems is a hallmark of a successful polycatenane synthesis and will be seen repeatedly throughout this review.

Polymerization of preformed molecular catenanes

Conceptually, the simplest way to synthesize a polycatenane is to first produce a catenane that is decorated with functionalities amenable to polymerization. The catenane then acts as a monomer or co-monomer in a conventional polymerization step. There are two key considerations that need to be made when employing this approach. Firstly, the exact nature and placement of the polymerizable groups is

important, as this will dictate the final polycatenane architecture. For example, it is possible to access poly[2]catenanes, pendant polycatenanes, and polymer networks with catenane crosslinks using this approach. Secondly, the chemical functionalities present in the catenane must not interfere with the polymerization chemistry (i.e., by acting as terminating or chain transfer agents) if high molecular polymers are to be achieved.

The first successful polycatenane synthesis using this approach was carried out by Geerts and coworkers, who prepared a range of poly[2]catenanes using the [2]catenane **3_H-Br** (R = Br) (Fig. 3a) as one of the monomer units.¹⁵ The small size of the macrocycles along with strong hydrogen bonding between the ring components in **3_H-R** renders them immobile, so that the [2]catenane is fixed into one of three potential conformational isomers, distinguished by the relative orientations of the aryl bromide groups: **IN-IN**, **IN-OUT**, and **OUT-OUT** (Fig. 3a). In practice only two of these isomers (**IN-OUT** and **OUT-OUT**) were observed, likely a consequence of steric effects hindering the formation of the third (**IN-IN**) isomer. The AABB polymerization of purified **3-Br IN-OUT** (AA) was subsequently conducted with a variety of (BB) comonomers, bis-alkyne **4a** (via Sonogashira coupling), bis-boronic acid **4b** (via Suzuki coupling) and **4c** and **4d** (via Stille coupling), yielding polymers **5a-d**, respectively (Fig. 3b). Poly[2]catenanes with up to 8 repeat units by mass spectrometry (*m/z* = 15,427) were reported. As might be expected given the lack of mobility in the monomeric catenanes, the interlocked rings in the polymer were similarly immobile, as confirmed by variable temperature ¹H-NMR which showed no change at elevated temperature. The authors did report a *T_g* value of 245 °C for **5b** but no further materials characterisation was conducted.

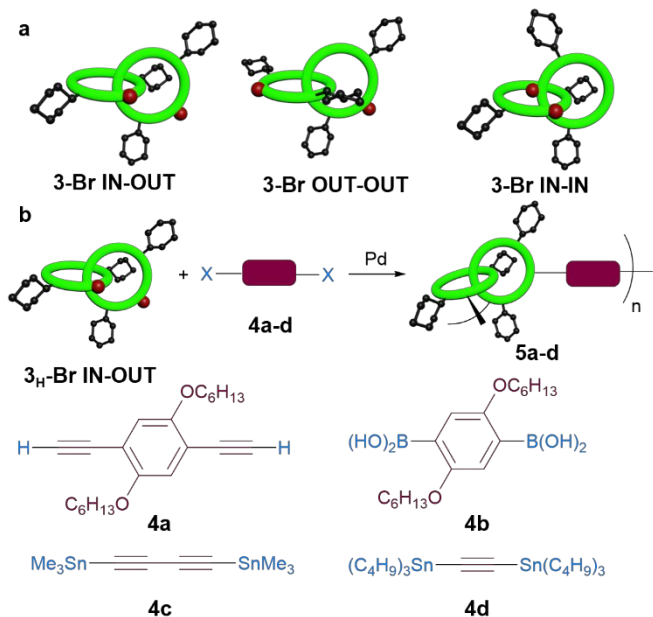


Fig. 3 a) The three isomers of the [2]catenane **3-Br** that are theoretically possible, however the **IN-IN** isomer is not observed. b) Synthesis of poly[2]catenanes **5a-d** by reaction of **3-Br IN-OUT** with comonomers **4a-d**.

Subsequently, the same authors prepared a poly[2]catenane with methylated amide units in order to remove the H-bonding within the catenane.^{48,49} Unfortunately, while the amide *N*-methyl groups eliminated intra-catenane H-bonding, these *N*-methylated [2]catenanes did not exhibit ring component mobility, as confirmed by variable temperature ¹H NMR experiments of the *N*-methylated **OUT-OUT** bisphenolic [2]catenane **3_{Me}-OH**. This bisphenolic [2]catenane was copolymerized with a diacid and the resulting poly[2]catenane had a number average degree of polymerization (*DP_n*) of 18 with masses up to 62,000 g/mol observed by matrix-assisted laser desorption ionization time-of-flight mass spectrometry (MALDI-TOF MS). Using gel permeation chromatography (GPC) and viscosity data (in THF), a relatively large Kuhn segment length of 44 Å was calculated, suggesting that this polymer exhibited an extended conformation, presumably on account of the rigid **OUT-OUT** [2]catenane segment. Unfortunately, the poly[2]catenane material was extremely brittle and demonstrated poor flow properties, hampering any mechanical studies.

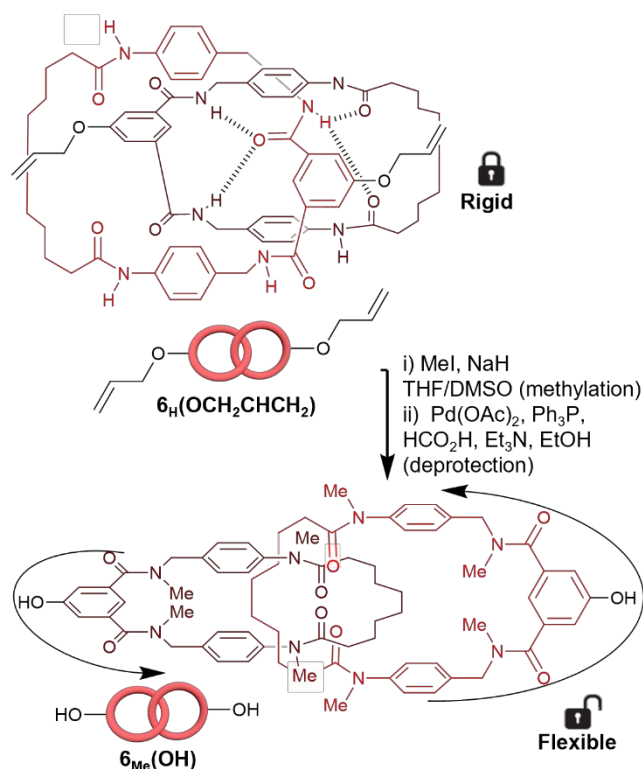


Fig. 4 Representation of the intra-catenane H-bonding present in the amide [2]catenane **6_H(OCH₂CHCH₂)**. Methylation of amide nitrogens in **6_H(OCH₂CHCH₂)** results in an increased mobility of the component rings. The phenolic derivative **6_{Me}(OH)** is prepared after a deprotection step. The subscript nomenclature throughout indicates the substitution at the amide nitrogens. Reproduced from Ref. 7 with permission from Springer Nature.

While successfully achieving the synthesis of poly[2]catenanes, the lack of mobility within the [2]catenane moieties incorporated into **5a-d** hindered an exploration of how the catenanes unusual mobility elements impact the polymer properties. To address this, new catenanes were designed and synthesized that had reduced steric bulk on the macrocycle.⁵⁰ In

particular, the amide-containing catenanes **6_H(R)** (Fig. 4) were prepared in a similar manner to **3** (Fig. 2c), utilizing H-bonding and π - π interactions to template their synthesis. While the presence of the amide hydrogen-bonding in **6_H** still hinders the mobility of the rings,⁵⁰⁻⁵⁴ methylation of the amide units in **6_H(OCH₂CHCH₂)** followed by deprotection of the phenolic OH groups yields the [2]catenane **6_{Me}(OH)** in which the rings were shown to be mobile. Using difunctional monomers based on this basic catenane, a range of polymers have been prepared. For example, a series of polycarbonates **7** ($M_n = 15,900, 9,900, 8,100$ g/mol) were prepared with varying amount of catenanes incorporated into the backbone by copolymerizing a bisphenol A polycarbonate (**BPA-PC**) oligomer ($M_n = 1,300$ g/mol) with 10, 20 or 30 wt.% of **6_{Me}(OH)**, respectively (Fig. 5a).^{50,51} The effect of the [2]catenane moieties on the properties of these polycarbonates was then assessed through dynamic mechanical analysis (DMA) experiments. While incorporating the catenanes into the **BPA-PC** backbone had little-to-no effect on the T_g of the material (T_g of **7** and **BPA-PC** ≈ 150 °C), a new thermal transition was observed at lower temperatures. DMA measurements of BPA-PC typically reveal two thermal transitions at -100 °C and 80 °C, termed γ and β transitions, that are assigned to cooperative motions of the polycarbonate segments, and defects or constraints in the film, respectively. Interestingly, in addition to these γ and β transitions, the 20 wt.% catenane copolymers of **7** exhibited a third sub- T_g thermal transition at *ca.* -6 °C. The researchers assigned this new relaxation to the catenane mobility, suggesting that catenane conformational changes and dynamics can indeed impact the polymer's material properties.

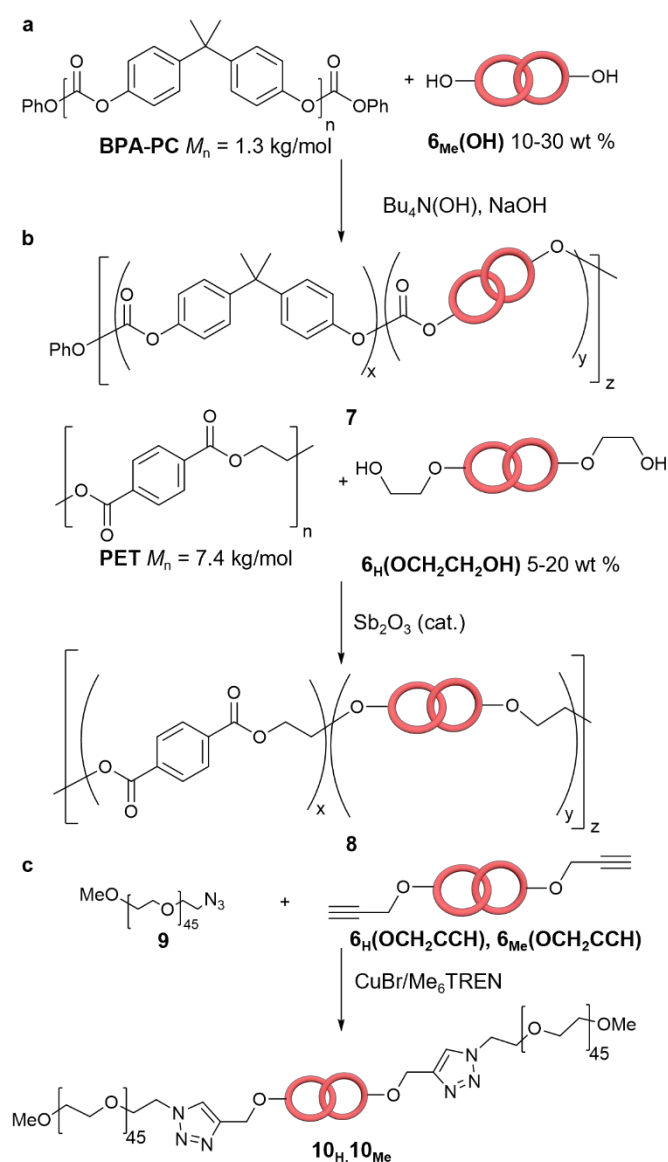


Fig. 5 a) Synthesis of the polycarbonate-based poly[2]catenane **7** from bis-phenol functionalized **6_{Me}(OH)** and polycarbonate oligomer **BPA-PC**. b) Poly(ethylene terephthalate)-based poly[2]catenane **8** was synthesized via transesterification of low molecular weight poly(ethylene terephthalate) with **6_H(OCH₂CH₂OH)**. c) Poly[2]catenanes **10_H** and **10_{Me}** that both contain a single [2]catenane moiety between poly(ethylene glycol) blocks were synthesized using click chemistry from **9** and the bis-alkyne functionalised catenanes, **6_H(OCH₂CCH)** and **6_{Me}(OCH₂CCH)**. Adapted from Ref. 7 with permission from Springer Nature.

Poly[2]catenanes based on poly(ethylene terephthalate) (PET) have also been prepared. In this case, the hydrogen bonded [2]catenane functionalized with two hydroxyethyloxy groups (**6_H(CH₂CH₂OH)**) was reacted with a low molecular weight PET pre-polymer ($M_n = 7,400$ g/mol) under transesterification conditions to access polymer **8** with 5, 10, or 20 wt% of catenane (Fig. 5b).⁵¹ In these poly[2]catenanes, the T_g of the copolymers increased as a function of catenane incorporation into the PET backbone, which is presumably a consequence of adding the more rigid, immobile catenane into the polymer backbone. It is also possible that the T_g increase

may also be a result of hydrogen bonding between the amide N-H's and the ester groups in the PET.

Using a similar basic amide-based catenane, Fustin and co-workers set out to explore if the incorporation of a single catenane moiety into a polymer backbone can result in changes in the overall polymer properties. Bis-propargyl [2]catenanes (**6_H**(OC₆H₁₂CH=CH₂) and **6_{Me}**(OC₆H₁₂CH=CH₂)) were therefore coupled to mono-azide terminated poly(ethylene oxide) **9** (PEO, $M_n = 2,000$ g/mol) using copper(I) catalysed azide-alkyne cycloaddition (CuAAC) click chemistry (Fig. 5c).⁵² The resulting polymers **10_H** and **10_{Me}** contain only a single [2]catenane moiety with PEO chains attached to each ring; studies were carried out to explore any differences between the polymer with a mobile [2]catenane (**10_{Me}**) versus the polymer with the immobile [2]catenane (**10_H**). In the non-polar solvent 1,1,2,2-tetrachloroethane (TCE), AFM-based single molecule force spectroscopy measurements showed that **10_{Me}** had a smaller persistence length (0.45 ± 0.05 nm) than the less mobile **10_H** (1.0 ± 0.15 nm), indicating that a single mobile mechanical bond can enhance polymer chain mobility. This was further supported by carrying out the same experiment in a hydrogen bond competing solvent, such as dimethylformamide (DMF), where both polymers had a similar persistence length (**10_H** = 0.50 ± 0.10 nm and **10_{Me}** = 0.45 ± 0.05 nm). A similar phenomenon was observed in a polymer containing a different central [2]catenane unit with each ring bonded to polystyrene ($M_n = 3,100$ g/mol). The [2]catenane in this polymer contained pyridyl units and, as such, the motion of the [2]catenane could be locked by adding Pd²⁺.⁵⁵ The metal-containing polymer exhibited a T_g of 120 °C while the metal-free

polycatenane had a T_g of 109 °C, which is 2 °C higher than neat polystyrene of a similar molecular weight.⁵⁵

The polycatenane synthetic method outlined above is not limited to linear polymers: the [2]catenane can also be incorporated into network structures.^{54,56,57} In one recent work, the amide-based catenane **6_H**(OC₆H₁₂CH=CH₂), featuring a vinyl group on each ring, was polymerized by acyclic diene metathesis (ADMET), end-capped by trityl sulfane, using Grubbs Generation II catalyst (Fig. 6a), and deprotected with trifluoroacetic acid (TFA) to yield the thiol terminated polycatenane **11** ($M_n = 3,200$ g/mol, $DP_n = 23$). The crosslinked polycatenane network, **12**, was then formed via the photochemical-induced reaction of **11** with the cross linker pentaerythritol tetraacrylate.⁵⁶ The amide-containing [2]catenanes will have limited mobility (and can be considered locked) unless the intra-catenane hydrogen bonding is disrupted (unlocked). Consequently, the stiffness and toughness of 1,2,4-trichlorobenzene gels of these poly[2]catenane networks could be significantly altered by conditions that disrupt the amide hydrogen bonding within the catenane, such as increasing the temperature of the gel or by adding acid to it. Fig. 6b shows that increasing the temperature of the gel to greater than 50 °C results in significant decrease of the Young's modulus and a concomitant increase in the strain-at-break. A similar change in properties can be observed upon adding trifluoroacetic acid to the gel (Fig. 6c). Cyclic tensile tests showed that the networks where the rings are locked had a much higher hysteresis than the unlocked ones, suggesting that the flexible [2]catenanes promote more efficient stress

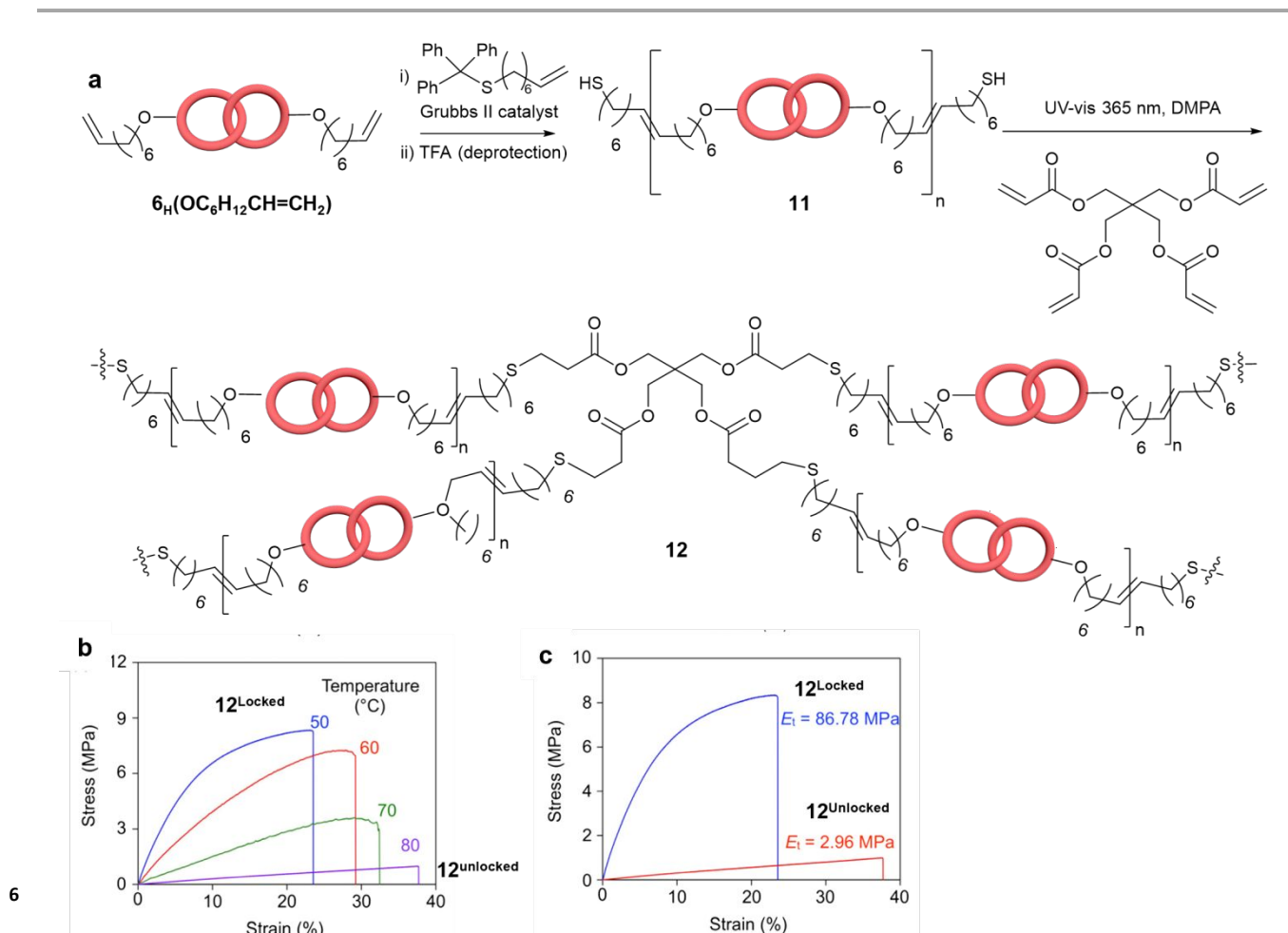


Fig. 6 a) Synthesis of the [2]catenane-containing network **12** by the reaction of dithiol **11** with pentaerythritol tetraacrylate. The effect of b) temperature (from 50–80 °C) and c) pH on the stress-strain behaviour of 1,2,4-trichlorobenzene gels of **12**. **12_{locked}** (blue curve), +TFA - **12_{unlocked}** (red curve). Reproduced from Ref. 56 with permission from Chinese Chemical Society.

relaxation.⁵⁶ Other [2]catenane-containing networks have also been prepared and exhibit similar trends: namely the properties are highly dependent on the mobility of the catenanes in the network.⁵⁴

Supramolecular polymeric networks that have [2]catenanes incorporated into their network structures have also been prepared. For example, the polystyrene-based random copolymer **13** ($M_n = 8,800$ g/mol) that contains secondary ammonium salts can be self-assembled with the [2]catenane crosslinker **14a** that contains two benzo[21]crown-7 units to yield the [2]catenane-containing supramolecular network **13·14a** (Fig. 7a). For comparison, a non-interlocked supramolecular polymer network system **13·14b** was prepared from **13** and a ditopic benzo[21]crown-7 species **14b** (Fig. 7b).

non-catenated systems in this study, it is difficult to assess the full impact of the mechanical bond on the properties of these assemblies.

Attaching preformed catenanes onto polymer backbones

Of course, there are ways for a catenane moiety to be incorporated into a polymer other than within its backbone, for example, as a side group or “pendant” to the backbone. Such pendant polycatenanes were first prepared by Stoddart and coworkers.⁵⁸ Early works in this area^{58,59} polymerized functionalized pre-formed [2]catenanes, similar to the methods discussed in the previous section. However, more recent efforts have focused on attaching the catenane side groups to an existing polymer backbone using the robust CuAAC “click”

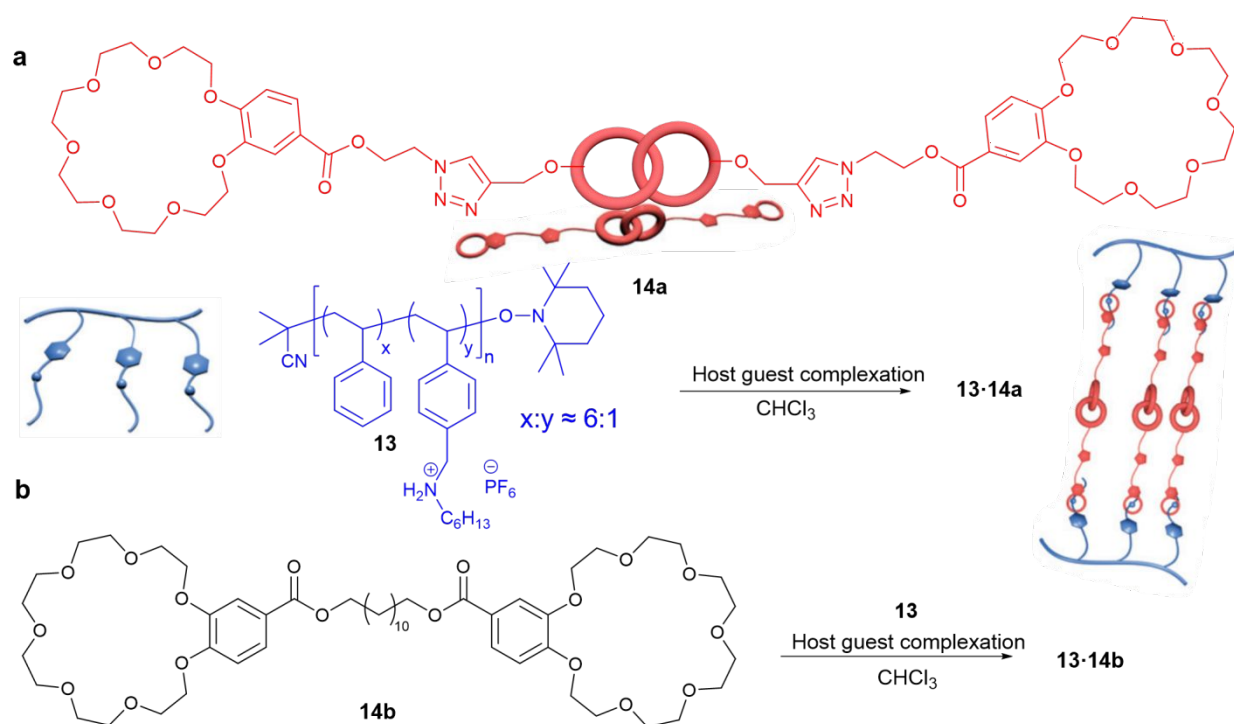


Fig. 7 a) Supramolecular network **13a·14** formed by the reaction of polymer **13** with [2]catenane **14a**. The crown ethers on **14a** crosslink via supramolecular interactions with the ammonium groups on **13**. b) Comparative non-catenated network **13·14b**, made by the self-assembly of **13** and **14b**. Reproduced from Ref. 57 with permission from the Royal Society of Chemistry.

While the specific viscosity of chloroform solutions of **13** show a linear increase with increasing concentration (1.0 – 7.0 mM), both **13·14a** and **13·14b** showed larger, non-linear increases in specific viscosities with concentration, consistent with the formation of a supramolecular polymer network. Notably, **13·14a** exhibits a larger specific viscosity than **13·14b** at similar concentrations, and rheological measurements revealed a higher storage and loss modulus (G' and G'') for **13·14a** (interlocked) versus **13·14b** (non-interlocked) at all frequencies. These findings are consistent with the higher rigidity of the **13·14a** supramolecular network, presumably on account of the rigid hydrogen bonded catenated rings, as opposed to the flexible alkyl chain in the **13·14b** network. Unfortunately, given the very different chemical composition of the catenated and

chemistry.⁶⁰ For example, Olson *et al*³⁹ reacted azide-functionalized polymethacrylate with an alkyne functionalized cyclobis(paraquat-*p*-phenylene), to yield the polymer **15** ($M_n = 6.1 \times 10^5$ g/mol) with the tetracationic macrocycle on the side-chain. Catenation of the side chain macrocycle was achieved under thermodynamic control (Fig. 2b), via iodide-catalysed nucleophilic substitution that opens and closes the cyclophane ring in the presence of the 1,5-dioxynaphthalene-based crown ether. The resulting pendant poly[2]catenane **16** had a M_n of 3.1×10^6 g/mol as determined by GPC-MALS (Fig. 8a).³⁹ Both **15** and **16** are polyelectrolytes with nonpolar backbones, leading to large ionic aggregates in solutions with the polar solvent DMF. However, the nature of these aggregates is quite different between the two systems. In particular, **15** forms large,

spherical aggregates in which the ionic groups form a shell around the solvophobic backbone. Meanwhile, the strong π - π stacking interactions between neighbouring pendant catenanes in **16** (Fig. 8a) lead to rod-like conformations, but also appear to disrupt aggregation, resulting in considerably smaller clusters. Unlike the previously discussed polymers, where the focus was primarily on taking advantage of the mobility elements present in individual catenane moieties to change the polymer properties, these materials derive the changes in their polymer properties via interactions between separate pendant catenanes.

The same CuAAC “click” chemistry was used to make the pendent poly[2]catenane **17** featuring the same tetracationic cyclophane ring interlocked with a crown ether containing both dioxynaphthalene and thiafulvalene electron rich groups (Fig. 8b). The synthesis of this pendant poly[2]catenane took a slightly different approach: the [2]catenane **18** was preformed and then attached to the polymer **19** ($M_n = 39,000$ g/mol, $\bar{D} = 1.4$) by reacting an azide side group on the parent polymer with the alkyne on the cyclophane ring. After **18** had reacted with **19** for 24h, excess methyl propargyl ether was added to react with any remaining azide groups. The resulting polymer **19** was found to have ca. 42 [2]catenane pendant units (as determined by NMR integration and GPC-MALS). As had been observed in similar small molecule [2]catenanes, the conformation of the pendant catenane could be switched by chemical or electrochemical stimuli (albeit at a slightly slower rate): when a two electron oxidation of the thiafulvalene group occurs, the tetracationic cyclophane ring moves from the thiafulvalene moiety to the dioxynaphthalene moiety, making **17²⁺** (Fig. 8c).¹⁶

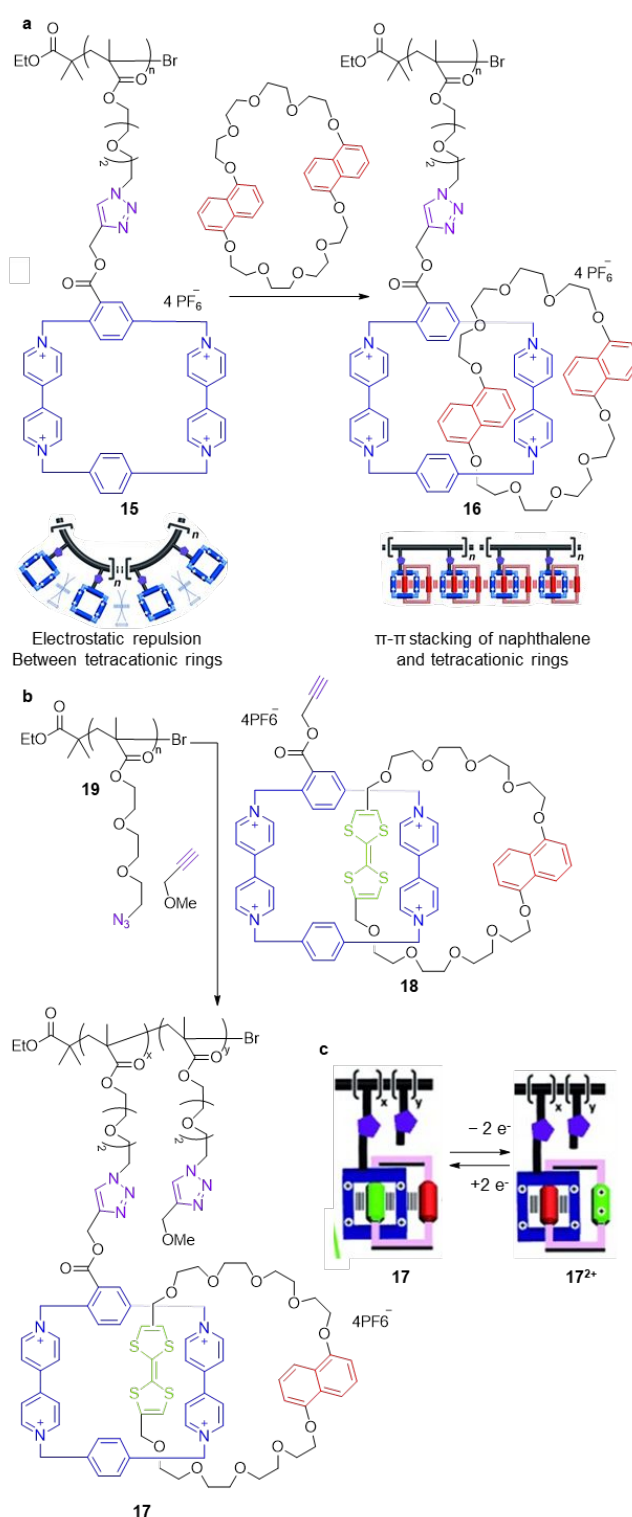


Fig. 8 a) Synthesis of the pendant poly[2]catenane **16** from the polymer containing the tetracationic cyclophane side groups **15**. Reproduced from Ref. 39 with permission from John Wiley & Sons, Inc. b) A second route to pendant poly[2]catenanes (**17**) by preforming the [2]catenane bearing an alkyne side group (**18**) and using azide-alkyne click chemistry to attach it to the polymer **19**. c) Switching of the cyclophane ring position from the thiafulvalene to the dioxynaphthalene moiety upon 2 electron oxidation of the catenane units in **17**. Reproduced from Ref. 16 with permission from John Wiley & Sons, Inc.

Ring expansion of small molecule catenanes

If the pre-formed [2]catenane structure undergoes a ring expansion, it is possible to access a polymeric [2]catenane,⁶¹ which are [2]catenanes (Fig. 1d) where one or more of the rings are polymeric. This architecture can be created by making a low molecular weight catenane that can take advantage of ring-expansion strategies (Fig. 9). To exploit such an approach the Advincula group targeted a tin-containing [2]catenane initiator **20**·Cu⁺, that was prepared using Cu(I)-phenanthroline templating followed by ring closing of the tetraethylene glycol substituents on the phenanthroline ligand with dibutylidimethoxytin.⁶² Ring expansion can be achieved by insertion polymerization of ϵ -caprolactone (CL) or L-lactide (LA) monomers yielding the catenated PCL (**21**-PCL) and (PLA **21**-PLA), respectively. The polymerization of **20**·Cu⁺ with PCL was shown to be living, allowing a variety of different molecular weights (11,500-40,100 g/mol of **21**-PCL) to be prepared by controlling the feed ratio of the catenane initiator to monomer. Comparison of the **21**-PCL to linear PCL of similar molecular weight showed that the polymeric [2]catenane had a lower melting point (44-49 °C vs 53-54 °C), lower degree of crystallinity (46 %-48 % vs 55-57 %), and a more compact crystalline structure (from wide-angle X-ray scattering). Such differences are consistent with the topological constraints inherent in the polymeric [2]catenane architecture that limit the segmental mobility of the polymer.⁶²



20·Cu⁺

- 1) Caprolactone or L-Lactide
- 2) KCN (demetallation)

= PCL (**21**-PCL) or PLA (**21**-PLA)

Fig. 9. Polymeric [2]catenane synthesis by ring expansion of [2]catenane **20**·Cu⁺ by insertion polymerization of caprolactone or L-lactide into the Sn-O bond of the [2]catenane to make **21**-PCL and **21**-PLA.

Catenation of linear polymers

Polymeric [2]catenanes can also be accessed from linear polymeric structures. This method of catenane synthesis generally requires a templated approach.⁶²⁻⁶⁷ For example, to access polymeric [2]catenanes, a phenanthroline derivative functionalized with two atom transfer radical polymerization (ATRP) initiator sites was complexed with Cu⁺ ions (Fig. 9).⁶³ The resulting 2:1 ligand:metal ion complex **22**₂·Cu⁺ was then used as a tetrafunctional initiator for the ATRP of styrene to yield the polymeric complex **23**₂·Cu⁺ (*M_n* = 6,400 g/mol of the complex). Ring closing of the polymer chains was achieved using an atom transfer radical coupling (ATRC) reaction under high dilution to yield **24**·Cu⁺ and, following demetallation with KCN, the polymeric [2]catenane **24** was obtained. Using this approach, it is also possible to access polymeric [2]catenanes in which the rings are cyclic block copolymers. For example, the polystyrene complex **23**₂·Cu⁺ can be used as a macroinitiator for the polymerization of methyl methacrylate. ATRC followed by metal ion removal yields the polymeric [2]catenane in which each ring is a cyclic poly(styrene-*b*-methylmethacrylate) (*M_n* of **24** = 5,900 g/mol).⁶⁴ This templated polymerization methodology can also be combined with other chemistries, for instance azide-alkyne click reactions can be used as the ring closing step.⁶⁵

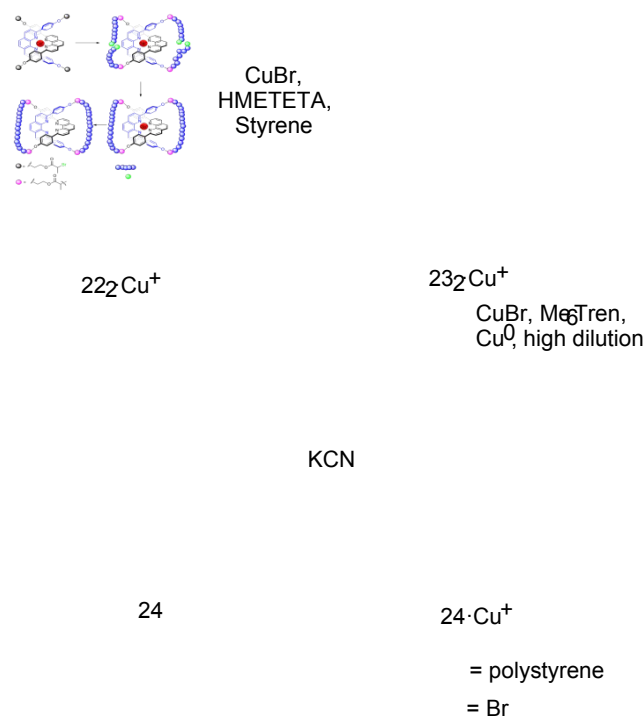


Fig. 10. Polymeric [2]catenane synthesis using a transition metal ion templating to yield a tetrafunctionalized initiator (**22**₂·Cu⁺) from which styrene is polymerized by atom transfer radical polymerization (ATRP). The bromide end groups of the polymeric assembly (**23**₂·Cu⁺) are coupled by atom transfer radical coupling (ATRC) resulting in the interlocked structure **24**·Cu⁺. The templating metal ion is removed using KCN to yield the polymeric [2]catenane **24**.

The prior examples employ the templating of molecular species and subsequent polymerization. However, it is also

possible to access polymeric [2]catenanes via templating and ring closing of pre-existing polymeric species. For example, Tezuka *et al.*⁶⁶ reported the use of electrostatic-induced self-assembly to prepare a polytetrahydrofuran (pTHF) based polymeric [2]catenane (Fig. 11). Using isophthaloylbenzylc amides for hydrogen bonding templating, a pTHF macrocycle was assembled with an appropriate linear pTHF derivative. To aid ring closing and the formation of the catenane, electrostatic interactions were employed in the form of ammonium-based cationic chain ends of the linear component and the ditopic counter ion biphenyl-4,4'-dicarboxylate. The polymeric [2]catenane **25** can then be formed via covalent fixation (*via* heat) of the assembly.

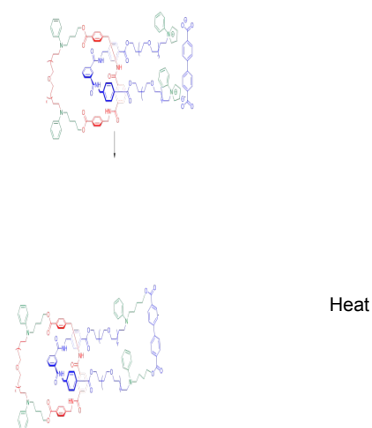


Fig. 11. Synthesis of polymeric [2]catenane **25** by cooperative electrostatic/hydrogen bonding self-assembly followed by a thermally-induced covalent fixing step.

Similar to the polymeric [2]catenane, a polycatenane consisting of multiple interlocked rings can also be formed using a linear polymer. These structures are known as a “radial” polycatenanes which, in their simplest form, are composed of one larger ring catenated with many smaller rings. Higashi *et al.* reported the synthesis of such polycatenanes via the ring closing of a pseudopolyrotaxane. A bis-thiol terminated symmetric triblock copolymer of PEG-PPG-PEG **26** was threaded with multiple β -cyclodextrins (β -CD) in aqueous solution, resulting in the pseudopolyrotaxane **26· β -CD. **26· β -CD was subsequently ring closed via thiol oxidation at high dilution using hydrogen peroxide to form the desired polymer **27** (Fig. 12a) with a M_n of *ca.* 18,000 g/mol and $\bar{D} = 1.05$ (GPC), which corresponds to the radial polycatenane with *ca.* 11 interlocked β -CD rings.²⁰ In addition to the radial polycatenane that contains the cyclic monomers of **27**, the GPC trace revealed higher molecular weight species that were assigned as the radial polycatenanes in which the large ring component is the cyclic dimer, trimer, etc., of **27** (Fig. 12b).****

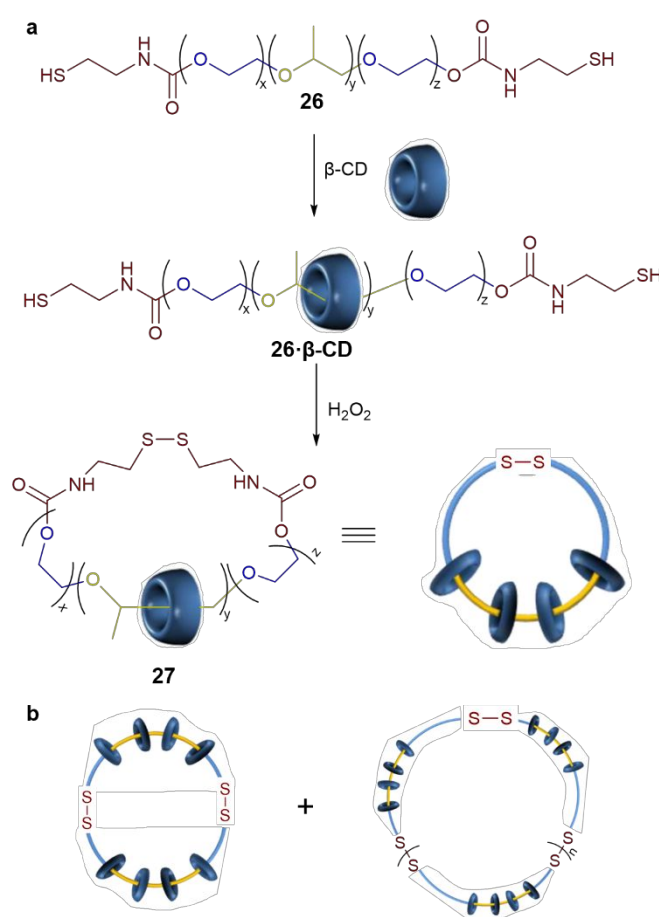


Fig. 12 a) Synthesis of radial poly[n]catenane **27**, formed by the threading of β -cyclodextrin rings onto a PEG-PPG-PEG triblock copolymer **26**. The ring closure of the pseudopolyrotaxane **26· β -CD is achieved via the oxidation of the thiol chain ends to yield **27** along with larger radial poly[n]catenanes that correspond to cyclic dimer and trimer of **26· β -CD. Reproduced from Ref. 20 with permission from Springer Nature.****

In a similar manner, the same group used diamine-terminated PEG-PPG-PEG and closed this β -CD-threaded polymer by reacting with terephthaloyl chloride.⁶⁸ The resulting radial polycatenane was determined (by ¹H NMR) to have *ca.* 11 β -CD. The threaded β -CD rings could be further functionalized in basic solvents while retaining the interlocked structure, thus establishing this system as a potential platform for engineering functional interlocked polymers.

Ring closing as the polymerization step

To access more complex catenated polymers, the separate steps of catenation and polymerization may need to be concerted. The primary materials created via this method belong to a special class of polycatenanes that are only comprised of interlocked rings. Such polymers have the potential to maximize the effect of the mechanical bond. An example of such a polymeric architecture is one in which the mechanical bond is incorporated as part of the polymeric backbone. The most fundamental such polymer is a linear poly[n]catenane, which is a linear polymer is made of consecutively linked rings, i.e., the molecular equivalent of a

macroscopic chain. The synthesis of such polymers is often challenging as they necessitate many ring forming reactions, which must all be performed in very high yield to achieve reasonable molecular weights.

Classical syntheses of [5] and [7]catenanes have been achieved using a stepwise approach where one or two rings are added in each step.^{47,69,70} Although these syntheses represent seminal achievements in the field of mechanically interlocked molecules, creating a poly[*n*]catenane with a higher number of rings (or degree of polymerization, DP_n) is challenging using such a stepwise approach. An alternative strategy⁷¹ sought to use Diels-Alder chemistry to polymerize monomeric [2]catenanes into a poly[2]catenane with cleavable 1,4-cyclohexadiene linkers. Conceptually, this approach could be used to design a poly[2]catenane where complete cleavage of the double bonds in the linker moiety (e.g., via ozonolysis) would result in a poly[*n*]catenane. However, this elegant method has not yet been utilized successfully.

Recently, the synthesis of linear (*l*-), cyclic (*c*-) and branched (*b*-) poly[*n*]catenanes has been achieved using a metallosupramolecular polymer (MSP) template.¹³ A 1:1 solution of ditopic macrocycle **28** and ditopic thread **29**, which both contain two 2,6-bisbenzimidazolylpyridine (Bip) ligands (Fig. 13a), were mixed with two equivalents of Zn^{2+} ions to yield the pseudopolyrotaxane metallosupramolecular polymer (MSP) **28-29-Zn²⁺** (Fig. 13b). Data suggested that the MSP was present in both the linear and cyclic form, the ratio of which depends on the reaction concentration.⁷² Ring closing the thread component in the MSP was achieved through olefin metathesis of its alkene tails resulting in a mixture that contains the metalated poly[*n*]catenanes. Removal of the metal ion yielded the desired poly[*n*]catenane **30**, along with some non-interlocked species. The interlocked products (obtained in ca. 75 % yield when the reaction was carried out at a thread (**29**) concentration of 2.5 mM) included linear, cyclic, and branched polymeric architectures with an average DP_n of 14 ($M_n = 21,400$ g/mol) (Fig. 14a). The *c*-poly[*n*]catenanes are presumably the result of complete ring closure of the thread components in the cyclic MSP. The data suggests that there are two different molecular weight populations of *l*-poly[*n*]catenanes⁷² which is consistent with *l*-**30** being formed from both the linear or cyclic MSPs (via incomplete ring closure of all the thread components). **b-30** is presumably formed by the intermolecular reaction between thread components in different MSPs which is supported by the fact that higher yields of the **b-30** is obtained at higher reaction concentrations.⁷² Fractionation (by preparatory-GPC) of the reactions mixture was undertaken to better determine the nature of the products. For the reaction carried out at 2.5 mM, the fractions with largest M_n consisted of *b*-poly[*n*]catenanes with up to 130 rings and an average of 55 rings (as determined by multiangle light scattering, MALS). The lower- M_n fractions comprised mostly linear and cyclic species,

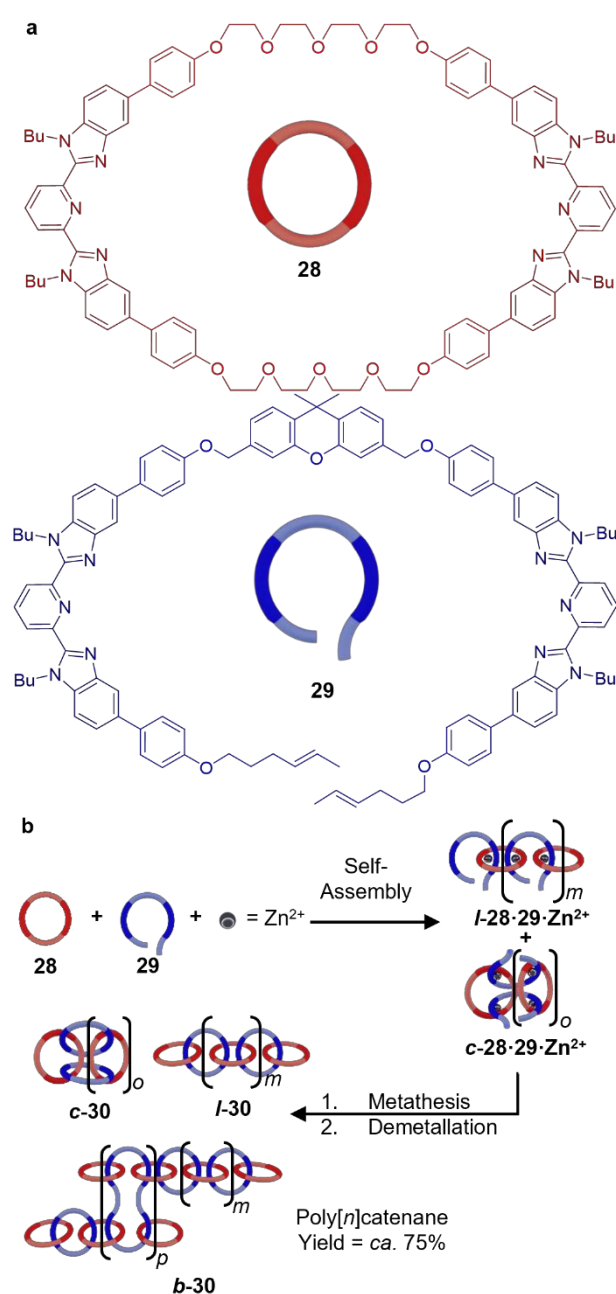


Fig. 13 a) Structure of ring (**28**) and thread (**29**) components used in the synthesis of poly[*n*]catenanes. b) The synthetic scheme to poly[*n*]catenanes starts with the formation of linear and cyclic metallosupramolecular polymers by the self-assembly of **28** and **29** (1 equiv. each) with Zn^{2+} (2 equiv.). Ring closing metathesis, followed by demetallation results in the formation of the poly[*n*]catenane **30** in a 75% yield. Reproduced from Ref. 72 with permission from the Royal Society of Chemistry.

with average DP_n of 12 and 8, respectively. Figure 14b shows how the distribution of these poly[*n*]catenane architectures in the final product is impacted by reaction concentration. At low concentrations, oligo, *c*-, and *l*-poly[*n*]catenanes dominated, while at higher concentrations (5 mM and 10 mM), the *b*-poly[*n*]catenane is the predominantly observed architecture. In these high concentration reactions, evidence from MALS suggests the presence of poly[*n*]catenanes with up to 640 interlocked rings (1,000 kg/mol).⁷²

As a consequence of the metal ion templating employed in the synthesis of the poly[*n*]catenanes, **30** exhibits stimuli-responsive behaviour. When the ligand moieties in these catenanes are not complexed to metal ions, the rings are mobile; however, adding in the metal ions results in the reformation of the metal–ligand complexes and a locking in of the catenane units. The *l*-poly[*n*]catenanes showed a 70% increase in hydrodynamic radius in solution (3.9 to 6.6 nm for a sample with a DP_n of 11) after metalation. This, combined with atomistic modelling data, supports the fact the highly flexible compact poly[*n*]catenane is converted into a semi rigid polymer upon metalation. The thermal properties of these polymer are also affected with an increase in T_g from 97 °C to >160 °C upon addition of Zn^{2+} .¹³

has been achieved through exploiting the π - π stacking and hydrogen bonding of **31**. **31** can self-assemble into hydrogen bonded supramacrocycles (termed rosettes, Fig. 15a). The π - π stacking of each rosette has a translational and rotational displacement leading to the formation of three-dimensional toroidal macrostructures, the nature of which can be controlled by judicious choice of solvent interactions, temperature, and reaction time. When the rosette monomer was added to a pre-formed toroid structure (Fig. 15a), the surface of the toroid served as nucleation points for the supramolecular assembly, leading to new rosette formations and subsequent assembly of a new toroidal structure that is interlocked with the nucleating initial toroid. The formation of these catenane-like superstructures was optimized by controlling the concentration of monomer **31** added to the solution and the number of interlocked rings could be increased by further monomer additions. AFM was used to directly visualize the system (Fig. 15b), revealing a nano-poly[22]catenane-like supramolecular assembly.⁷³

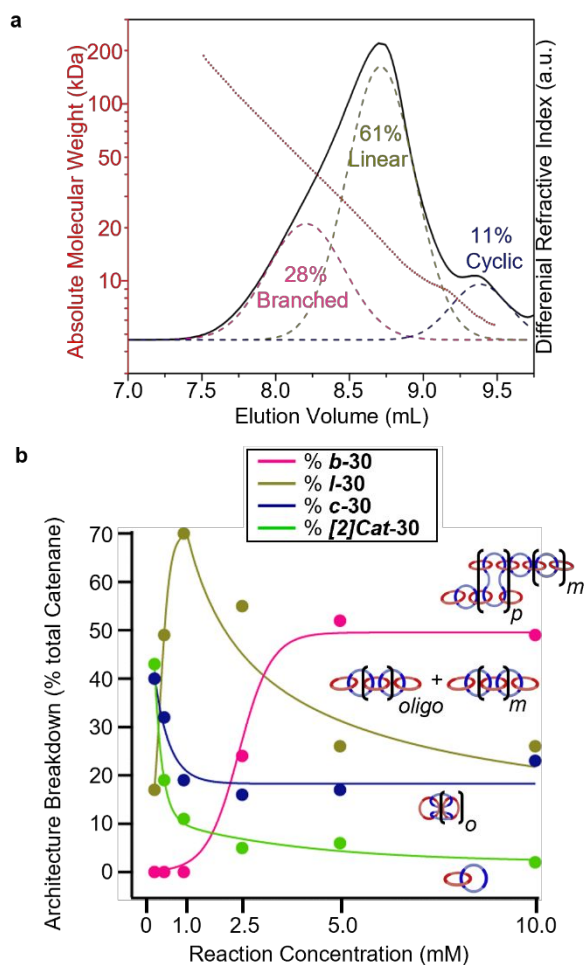


Fig 14. a) GPC trace of a purified poly[*n*]catenane reaction where the ring closing metathesis reaction is performed at 2.5 mM (w.r.t. **29** within the MSP). Deconvolution of the GPC trace and analysis of products by fractionation revealed branched, linear, and cyclic architectures. Reproduced from Ref. 13 with permission from American Association for the Advancement of Science. b) Graph showing the effect of concentration (w.r.t. **29** within the MSP) of the ring closing metathesis reaction on the crude product distribution of poly[*n*]catenanes. Reproduced from Ref. 72 with permission from the Royal Society of Chemistry.

While not poly[*n*]catenanes made from the interlocking of covalent macrocycles, it is worthwhile mentioning here that the formation of supramolecular poly[*n*]catenane-like assemblies

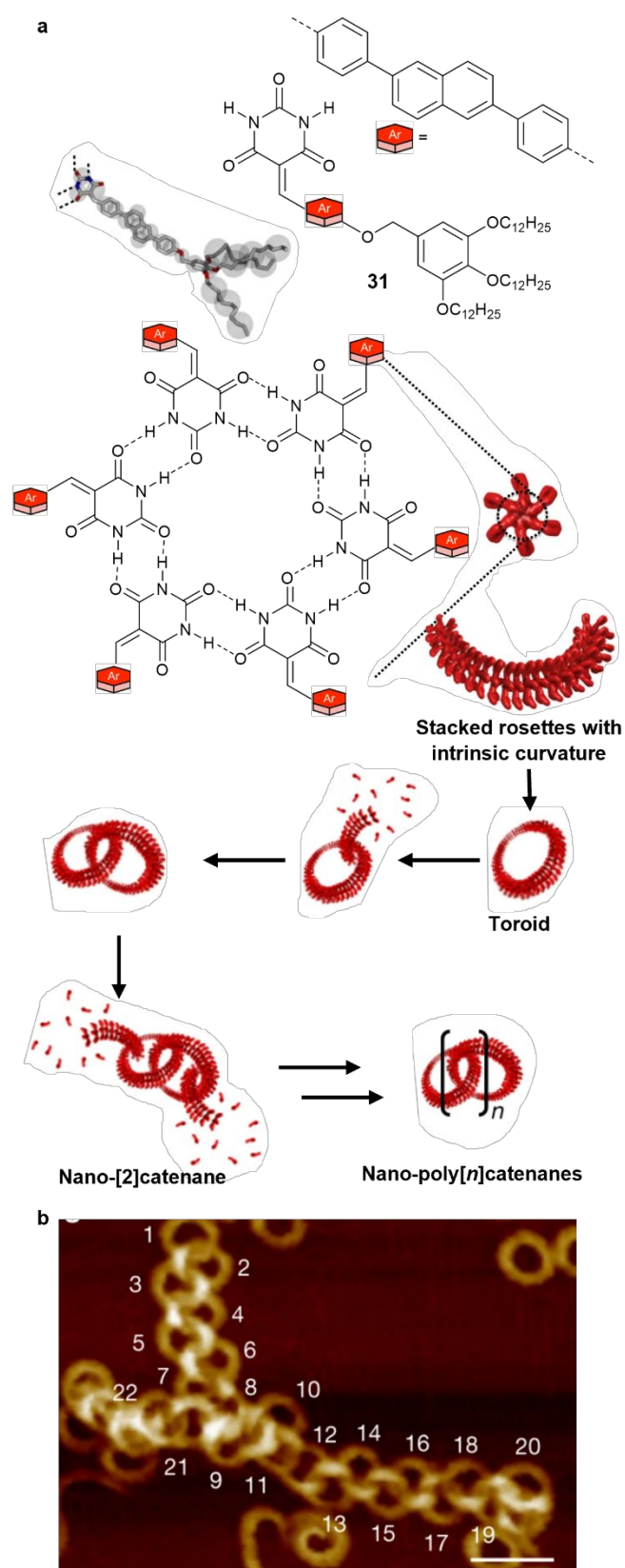


Fig. 15 a) Structure of building block **31** and its self-assembly into hydrogen bonded rosettes which subsequently assemble in toroids. These toroids can act as nucleation points for the formation of new toroids resulting in interlocked assemblies. b) AFM image of nano poly[n]catenanes with up to a [22]catenane being observed. scale bar = 50 nm. Reproduced from Ref. 73 with permission from Springer Nature.

Beyond cyclic, linear or branched poly[n]catenanes are network structures that consist of only interlocked rings. Such systems, the so-called Olympic gels, have actually been considered by polymer physicists for several decades;⁷⁴ however, the synthesis of such a material is a major challenge. While several semi-controlled statistical strategies have been suggested over the years, these methods have not proven fruitful.^{75–77} On the other hand, certain *uncontrolled* reactions, which involve simultaneous polymerization and catenation, have yielded catenated networks, albeit with a broad distribution of products.

The first such report to access network poly[n]catenanes, albeit it as a side product, resulted from the bulk polymerization of 1,2-dithiane.⁷⁸ 1,2-Dithiane was placed in a sealed reaction vessel under vacuum and reacted at 32 °C. While this polymerization yielded the desired small molecular weight cyclic polymer **32**, researchers also observed a small amount of a larger molecular weight material with unusual properties (Fig. 16a). This material exhibited a storage modulus that remained constant above its melting temperature (T_m ca. 44 °C) forming a rubbery plateau up to ca 100 °C, consistent with the formation of polymeric network. The linear polymer analogue, prepared by a similar thermal polymerization of 1,2-dithiane with the presence of a small amount of benzyl mercaptan as a chain terminator, showed a similar melting point but flowed above melting. Additionally, stress-strain experiments revealed that the new material was extremely flexible and elastic and could be stretched to 3,000 % elongation without breaking under load and underwent instant recovery. Under these same conditions, the linear polydisulfide broke at 800 % strain. On account of the unusual property profile of the higher molecular weight sample, it was tentatively labelled as a catenated network, **33**, where the polymerization and catenation happen simultaneously.⁷⁹ Since this initial report, thermal initiation of cyclic disulfides has been used to synthesize interlocked polymers with similar properties. Examples include polymers with aromatic sidegroups⁸⁰ and a copolymer of dithiane and lipoic acid.⁸¹ Recent efforts have detailed the ring expansion polymerization of cyclic disulfides, bearing an additional supramolecular moiety on each ring to make a charge transfer complex between rings, thus promoting catenation.⁸² The synergy of supramolecular interactions coupled with reversible bonds seems an attractive methodology for the formation of these materials, particularly in systems where the supramolecular interactions, and thus material properties can be modulated by external stimuli.

In a recent advance, Skov and coworkers were able exploit different chemistry to access catenated networks. In this work, α -monovinyl- ω -monohydride telechelic polydimethylsiloxane (PDMS) macromonomers of varying molecular weight (4, 15, 27 g/mol) were polymerized via a Pt-catalyzed hydrosilylation reaction in the bulk at 80 °C.⁸³ Here, the linear macromers can either react intramolecularly to form closed rings or intermolecularly to create larger linear strands, which may in turn undergo intra or inter-molecular reactions (Fig. 16b). The purity of the reactants and the exceptional efficiency of the reaction ensures that only a very limited number of chain ends remain after the reaction is complete. The result is a dispersed mixture

of catenated rings forming a network and small isolated unlinked rings or catenanes (Fig. 16c) which could be extracted by washing the material. After washing, the resulting networks were much softer and more extensible than comparable covalent PDMS networks formed by crosslinking macromonomers of the same molecular weight. For instance, the most durable catenated materials withstood strains of well over 1000% and exhibited a Young's modulus of roughly 0.01 MPa, while the covalent elastomers showed strain-at-break of less than 150% and modulus of ~0.27 MPa. Furthermore, the stress-strain response of the catenated networks at small (<50% strain) and large (> 50% strain) deformations could not be captured simultaneously by classical rubber elasticity theories; rather, a "slip-link" model was required to describe the data (Fig. 16d). This model incorporates stress relaxation at large deformations associated with the sliding of entanglement points. The contributions of the permanent (crosslink) and sliding elasticity were on the same order of magnitude for all catenated systems, indicating that the ability of the catenated rings to slide along each other is a key mechanism of stress relaxation. In contrast, covalently crosslinked control systems did not exhibit this mechanism, as inter-chain entanglements contributed only weakly to the material response that was dominated by the covalent crosslinks.

Despite the challenges in preparing synthetic Olympic gels, similar materials have in fact been observed in nature in kinetoplast DNA,^{84–87} which contain thousands of interlocked DNA rings (Fig. 17a). Here, nature cleverly circumvents the difficulties mentioned above through the use of topoisomerase enzymes which precisely cut and mend DNA segments, thereby relieving topological constraints. In recent years, researchers have begun to adopt this same approach to access DNA-based Olympic gels.^{88,89} For example, the appropriate enzymes (Human topoisomerase II- α or *E. coli* Topoisomerase I) are added into a concentrated cyclic DNA solution, allowing the rings to cross one another to obtain a topological equilibrium. This system is effectively a dynamic catenated network with temporary links between rings. If the enzymatic activity is arrested (for example by titrating ethylenediaminetetraacetic acid (EDTA)), the topology is frozen in this highly interlocked state since the segments can no longer pass through one another.^{90,91} As one might expect, the rheological behaviour of the dynamic and permanent networks exhibited pronounced differences. Although both systems showed an elastic plateau at intermediate times (i.e., shorter than the characteristic timescale for enzyme activity), at longer times the dynamic network demonstrated terminal flow behaviour typical of uncrosslinked polymer solutions while the static network remained elastic (Fig. 17b). Thus, by promoting or restricting the activity of topoisomerase, one can switch these systems between solution-like and gel-like states, respectively.

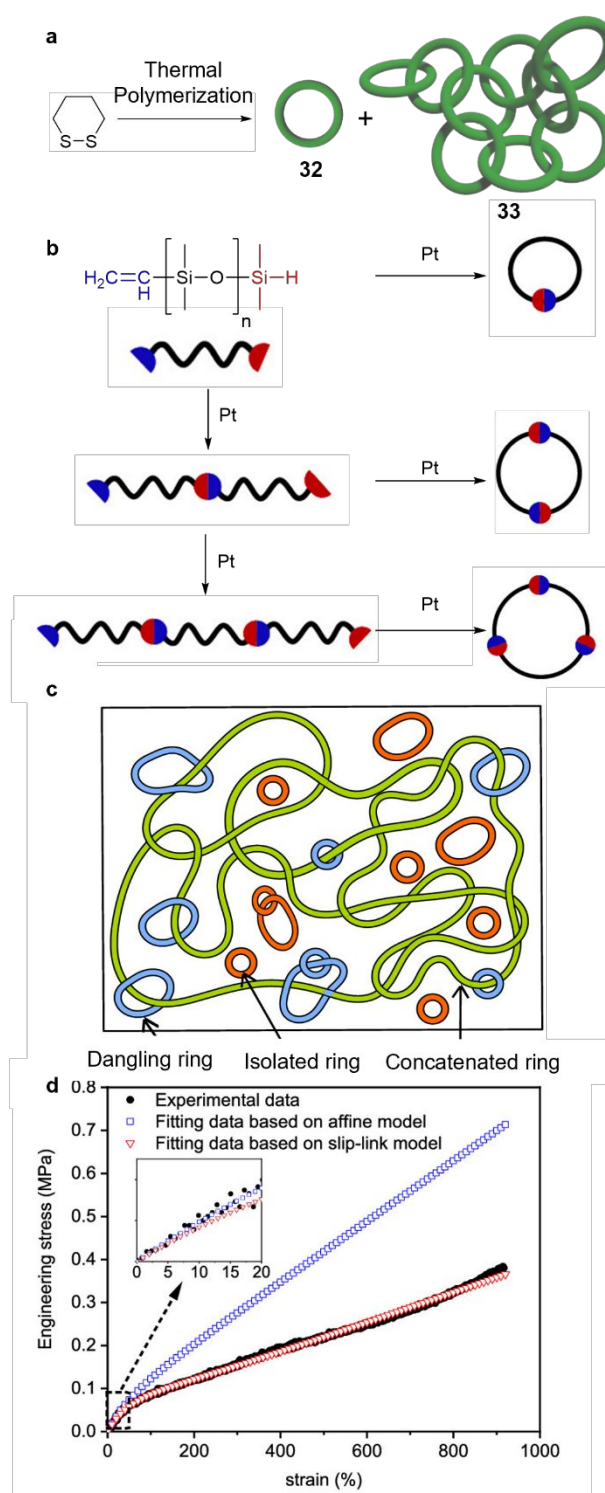


Fig. 16 a) The thermal polymerization of 1,2 dithiane resulting in the formation of large rings **32** and catenated networks **33**. Reproduced from Ref. 7 with permission from Springer Nature. b) Synthesis of polydimethylsiloxane (PDMS) rings using a platinum catalysed hydrosilylation reaction and c) an illustrated depiction of the ring structures formed in the synthesis, featuring a network of concatenated rings (green) in addition to catenated "dangling" rings not adding elasticity to the network (blue) and free isolated rings and small catenanes (red) not attached to the network architecture. d) Stress-strain curve for the PDMS-based catenated ring network demonstrating the failure of classical affine model at large deformations, while the slip-link model accurately describes the material response at all strains (Inset: detail of small-strain region). Parts b, c, d reproduced from Ref. 83 with permission from American Chemical Society.

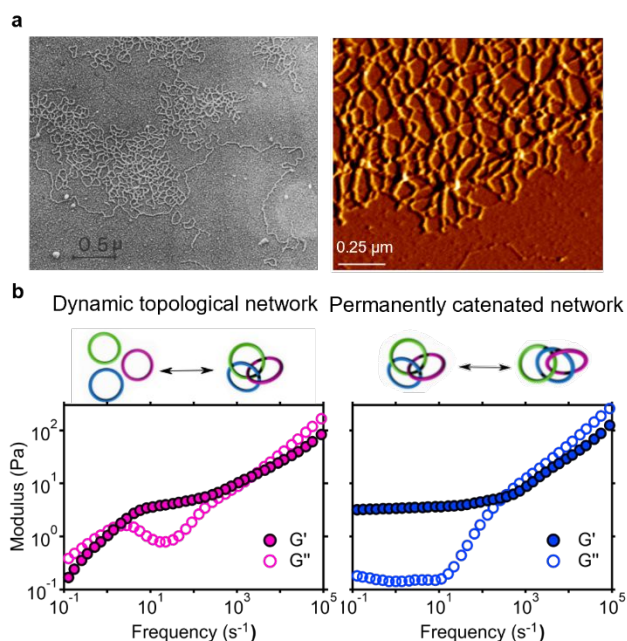


Fig. 17 a) AFM images of kinetoplast DNA, revealing its interlocked structure. Left image reproduced from Ref. 84 with permission from National Academy of Sciences. Right image reproduced from Ref. 85 with permission from Elsevier b) Storage and loss modulus of an Olympic gel, formed from circular DNA and topoisomerase. Measurement is performed using dynamic light scattering micro rheology. The system behaves as an entangled polymer solution when the topoisomerase enzymes are active and therefore relax topological constraints in the system (left). When enzyme activity is inhibited (right) the system exhibits an elastic plateau at low frequencies, indicating a permanent network structure. Reproduced from Ref. 91 with permission from American Physical Society

Polycatenane properties: a physical point of view

The past decade has witnessed a dramatic growth in the research interest surrounding the physical properties of polycatenane polymers and their resulting materials. This interest is driven partly by the advances in synthesis described above, but also by the importance of linked structures in certain biological systems,^{92,93} as well as the close connections with the physics of ring polymers.⁹⁴ In this section, the theoretical foundations of the field and the connections with other areas of polymer physics will be touched upon. In contrast to the prior section the focus here will be on the underlying physical concepts, rather than the specific polymer topologies *per se*. As this section is generally architecturally agnostic, the focus is on providing a concise yet self-contained account of the field that is motivating to chemists, physicists, and engineers alike.

Since polymers have a great many available conformations, the study of their physical properties is invariably the domain of statistical mechanics.^{74,95} Polycatenanes are no exception in this regard, but the situation is much more complex than for ordinary linear polymers because the mechanical bond is inherently topological in character. The first attempt to incorporate such topological constraints in a statistical theory of polymers was carried out by Edwards over 50 years ago.^{96,97} In these pioneering works, he established a rigorous formulation of the problem in terms of topological invariants

and obtained some analytical solutions for simple model systems. Edwards' formulation served as the foundation for a bevy of theoretical works on polymer topology and linking which have yielded several interesting results, with applications in rubber elasticity and polymer dynamics.^{98–108} Similar approaches have also been applied to the study of catenated polymers, i.e. polymeric [2]catenanes and poly[*n*]catenanes.^{109,110}

In general, the goal of such works is to obtain the configurational distribution function of the polymer, which can be used to determine the polymer dimensions and their dependence on molecular weight, as well as material elasticity under certain simplifying approximations.⁹⁵ Although the mathematical description of polycatenanes is reasonably well formulated, the resulting equations are typically intractable and cannot be directly solved, even for the generic Gaussian chain model, which neglects all direct interactions between repeat units. Moreover, a connection to dynamical phenomena in the presence of such constraints is entirely lacking, hence the use of phenomenological models to describe entangled polymer dynamics.¹¹¹ In light of these challenges (and those pertaining to the chemical synthesis), much of the progress in understanding polycatenane properties is a result of molecular simulations, which were performed for polymeric [2]catenanes as early as 1975.¹¹² With the enormous advances in computing power over the last several decades, larger and more complex catenated systems have been brought within reach of computational scientists and a great deal of new insight has been gained in the last few years. These findings may be broadly grouped into three main areas: polymer size and scaling, elasticity, and dynamics and rheology, which will be discussed in turn.

On Matters of Size

The most basic physical property of a polymer is its size. This quantity (usually taken as the radius of gyration) depends on a variety of parameters, including molecular weight, flexibility, solvent quality, architecture, and more. Thus, when studying a new polymer architecture, the first step is typically to measure the size of the molecule and how it scales with molecular weight. For polycatenanes, there are several relevant quantities to consider. One set of quantities to consider are the dimensions of the individual rings within a polycatenane and how these scale with ring size (i.e., molecular weight) and number of threadings/catenations.

To begin, polycatenanes in solution can be considered. In general, molecular simulations have demonstrated that, in this respect, catenated rings behave much the same way as ordinary cyclic/ring and linear polymers. If the degree of polymerization of the ring is denoted as *m*, it is found that the size of the ring scales as, $r \sim m^{\nu}$ with $\nu \approx 0.588$ in good solvent conditions and $\nu = 1/2$ in theta solvent conditions, just as in ordinary ring and linear chains (Fig. 18a).^{113,114} Despite the comparable scaling, catenated rings are swollen compared to their unthreaded counterparts, with statistical segment lengths increasing by roughly 10%; this swelling ratio grows as the number of

catenating rings, N_L , increases with a form that appears universal (Fig. 18a inset). Also of interest is the observation that the number of threadings raises the theta temperature of these rings. It has been suggested that the threading segments act as additional points of attraction, which promote ring contraction at lower temperatures.¹¹⁴ Thus, topological linking (the presence of mechanical bonds) causes the rings to expand in good solvent conditions, but may also aid collapse in poor solvents. Linking also affects the shape of the rings, with catenation leading to less prolate structures (on average), even in the limit of infinite molecular weight.¹¹⁵

In the melt state, the situation is more complicated: the scaling exponents associated with ring size appear to be much smaller for linked rings than unlinked ones (as low as $\nu = 0.38$), even though the linked species are still swollen in terms of the effective segment length or characteristic ratio.¹¹⁶ It is believed that a complex interplay between intra- and inter-molecular topological interactions is responsible for this observation, however the situation is not entirely clear as simulations have not yet been conducted with rings large enough to reach limiting behavior.¹¹⁶

Rather than focusing on the size of the constituent rings the size of the entire polycatenane, R , can be considered. In this case, the size has a dependence on both m and n , with n being the number of rings in the polymer, with a general form $R \sim m^\mu n^\nu$ (μ being another scaling exponent). Clearly, the size of the polymer depends on the specific polycatenane architecture, but it is illustrative to focus on linear poly[n]catenanes, which both optimizes the effect of the mechanical bond while also being conceptually simple given the overall linear structure. Focusing on the polymer as a whole, it is perhaps unsurprising that the asymptotic scaling properties are identical to those of ordinary linear polymers, as these relationships are generally universal. Molecular simulations suggest the same scaling behaviour as given above for individual rings: $\nu \approx 0.588$ in good solvent conditions and $\nu = 1/2$ in theta solvent conditions and the melt (Fig. 18b).^{113,114,116,117} These results hold when considering both the radius of gyration and the end-to-end distance, whose distribution becomes Gaussian as the chain grows longer (Fig. 18b, inset). While some authors¹¹⁴ suggested that the scaling exponent, μ , of poly[n]catenanes in good solvent with respect to the ring degree of polymerization, $R \sim m^\mu$, was in fact somewhat larger than the values for ordinary polymers, $\mu = 0.64$, more recent simulations with larger rings suggest that the true asymptote is the standard $\mu = 0.588$, but with finite-size corrections that grow as the number of rings is increased.¹¹⁷ It is also worth noting that certain side-chain polycatenanes can exhibit dramatic changes in solution behaviour upon catenation, as discussed earlier.³⁹ However, it seems likely that these effects are driven not by the presence of catenation *per se*, but rather arise due to the combination of electrostatic, hydrophobic, and π - π stacking interactions inherent in the particular catenane and polymer system.

Yanking your chain

Topological interactions play a key role in the elasticity of polymer materials. Hence, one would expect polycatenane materials to exhibit unique or remarkable mechanical properties. Similarly, this will depend significantly on the specific architecture and crosslinking mechanism, as well as on the length scale of the mechanical bond, i.e., the ring size. As an example of the latter consideration, one would expect that a cross-linked poly[n]catenane network composed of nanometer-scale macrocycles (cf. Fig. 13) will behave quite differently from an Olympic gel comprising many very large interlocking ring polymers (cf. Figs 16 and 17). The available literature (almost entirely computational or theoretical) suggest that the former case is fairly pedestrian, as might be expected from the previous section. Indeed, for linear polycatenanes (whether poly[n]catenanes, poly[2]catenanes and other related species) their long length scale phenomena are qualitatively the same as those of other linear polymers, but with different numerical coefficients.^{110,116} In particular, the end-to-end vector in poly[n]catenanes is Gaussian distributed; this key property is directly related to network modulus in the classical theory of rubber elasticity. As a result, no anomalous elasticity is expected in such systems, at least at longer length scales. If the catenated segments are both prevalent and relatively short, unique finite size effects may become important. In these cases, molecular dynamics simulations have shown that an extensible worm-like chain model is applicable,¹³ and such effects may be incorporated into elastic theories in a mean field sense.¹¹⁸

As the rings become larger, for instance in polymeric [2]catenanes, the topological aspects become more important. This architecture has been a subject of interest for several decades as such systems can be experimentally produced with cyclic DNA.^{119,120} Moreover, it is the simplest interlocked system that can be treated using the powerful tools of polymer physics and field theory.^{96,97,109,121,122} Such methods suggest that a pair of entangled polymer rings should exhibit two distinct regions of elastic behaviour when stretched, both of them distinct from the Hookean behaviour of ordinary Gaussian polymers.¹²³ At small deformations, the catenane is completely deformable (zero modulus) up to an extension comparable to the size of the rings, r_g . At larger deformations, the free energy of the catenane, F , stretched to a distance r scales as $F \sim (r/r_g)^4$. This scaling relation suggests a modulus that increases as the strain squared. However, recent simulations did not observe any qualitatively different behaviour between polymeric [2]catenanes and isolated ring polymers,¹²⁴ although this is not necessarily surprising: theoretical models typically assume no excluded volume interactions, only topological restrictions, but simulations require an excluded volume force to maintain the topology. Moreover, it is not clear that the rings that have been simulated thus far are large enough to probe the asymptotic limits. In short, the situation remains unclear, as a complicated interplay of excluded volume and finite size effects seem to obfuscate the asymptotic behaviour; further research on such systems is desirable as they are the key components of more complex systems such as Olympic gels.

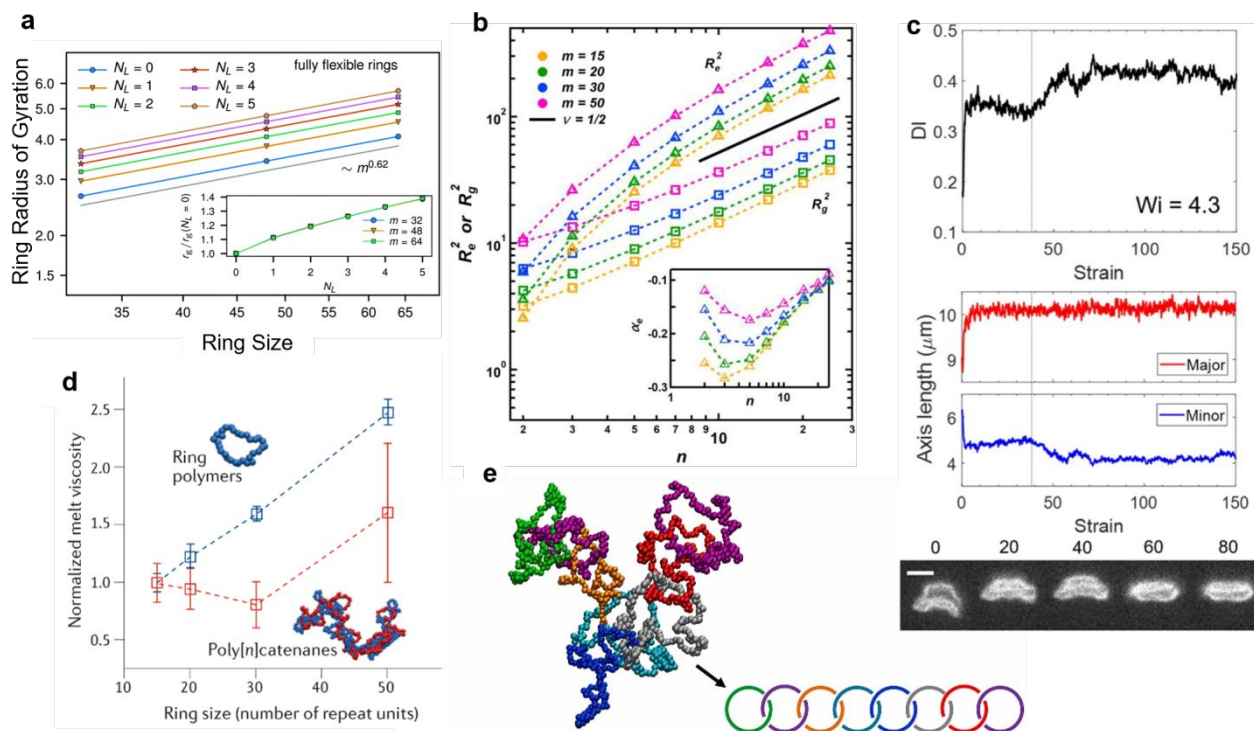


Fig. 18 a) Dependence of ring radius of gyration on ring size for catenated rings with N_L linked rings in good solvent conditions. The scaling exponent is close to the standard value of $\nu \approx 0.588$. Inset: Swelling of rings relative to unlinked state. For all ring sizes, the same dependence on N_L is observed. Reproduced from Ref. 114 with permission from the Royal Society of Chemistry. b) Radius of gyration and end-to-end distance of poly[n]catenanes in the melt as a function of the number of rings, n , and the ring size, m . For large polymers, the random walk scaling $R \sim n^{1/2}$ is recovered. Inset: A non-gaussian parameter for the distribution of end-to-end distances. At large n , the polymers approach the ideal limit at zero. Reproduced from Ref. 116 with permission from American Chemical Society. c) Deformation response of kinetoplast sheets in elongational flow. A folding event of the membrane takes place at an absolute strain of 40 times. Reproduced from Ref. 92 with permission from National Academy of Sciences. d) Normalized viscosities of ring polymer and poly[n]catenane melts as a function of the ring size. The poly[n]catenanes exhibit a nonmonotonic dependence on the ring size not seen in other polymer architectures. Reproduced from Ref. 135 with permission from AIP Publishing e) Visualization of a simulated poly[n]catenane. Reproduced from Ref. 134 with permission from Elsevier.

Olympic gels and other catenated networks were first suggested by de Gennes many years ago⁷⁴ and are expected to exhibit complex elastic properties. In particular, scaling arguments suggest a regime of zero modulus at small deformations and non-Hookean elasticity at larger strains.¹²⁵ In the latter case, the elastic force, f , scales with the deformation, λ , as $f \sim \lambda^{2/5}$. The accuracy of these particular conjectures has not yet been established, but synthetic catenated networks have indeed shown exceptional softness and extensibility, which can be directly attributed to the ability of the “crosslinks” to slide freely along the rings.^{79,83} Although these materials show great promise as novel elastomers, their synthesis relies on statistical linking between rings during the polymerization and the networks have large dispersities with respect to the ring size, making it difficult to grasp the underlying physics.

Somewhat more well-controlled networks can be obtained using the biosynthetic strategies described earlier, which can be carried out with mono-disperse DNA rings.^{90,91} Since these systems require a great deal of precious material, their mechanical properties are usually studied by micro-rheological techniques rather than traditional rheometry. Thus, although the linear viscoelastic behaviour has been characterized (and is not particularly remarkable), there is no solid understanding of

the stress-strain behaviour of these networks or how it is affected by the conditions of gel preparation. In this regard, simulations may be a valuable tool. Indeed, some researchers have already examined the swelling of model Olympic gels using lattice models; although this is not a direct study of the elastic moduli of the gels, the swelling ratio is indeed a closely related quantity, as it is controlled by the balance between osmotic pressure and network elasticity.⁹⁵ The key finding is that Olympic gels exhibit qualitatively different behaviour compared to ordinary covalent networks.^{77,126,127} In particular, gels made of longer rings exhibit a smaller equilibrium swelling, an unusual phenomenon that has a complex topological origin in the balance between catenation and traditional entanglement. For more direct investigations of the mechanical properties of Olympic gels, off-lattice methods have been recently proposed and offer a promising strategy for simulating these systems.¹²⁸

Another polycatenane system of particular interest is the kinetoplast, a natural occurring two-dimensional “sheet” of interlocked rings with a high intrinsic curvature.^{84,86,87,129} In recent years, Doyle and coworkers have performed extensive experiments on these systems^{92,130–132} and have observed a complex step-wise deformation response associated with large-scale folding events in the membrane (Fig. 18c).⁹² These

materials constitute intriguing and potentially illuminating models for studying catenated materials. However, these systems are not free from some of the challenges mentioned above; in particular, the rings of kinetoplasts are bi-disperse with a complex topology.

Go with the flow

Polycatenanes have long been sought after by synthetic chemists under the supposition that these polymers would exhibit unusual dynamical and rheological properties.⁷ Although such a hypothesis is well justified on the grounds that polycatenanes comprise many topologically interacting species, no specific predictions had been made until very recently. Using molecular simulations, the dynamics of polycatenanes in solution, the melt, and under nanoscale confinement have been studied and a consistent picture of their kinetic properties has begun to emerge. Specifically, the mechanical bond causes a slow-down in dynamics at the length scale of the overall ring – no matter how large. For instance, in solution, the overall ring relaxation in poly[*n*]catenanes is an order of magnitude slower compared to free rings, whether the ring contains ten repeat units or a hundred.¹¹³ These same results hold for poly[*n*]catenanes in the melt¹¹⁶ and for polymeric [2]catenanes in solution, and are essentially unaffected by the inclusion of hydrodynamic interactions.¹³³

The dynamical effect of the mechanical bond extends beyond the single ring scale. This is most apparent in poly[*n*]catenanes (Fig. 18e),¹³⁴ in which a clear separation between ring-like and chain-like dynamics is observed, leading to multiple sub-diffusive regimes in the monomer mean-squared displacement, even in the absence of reptation behavior.¹³⁵ However, this clean separation fails to account for the unusual rheological behaviour of these systems: the viscosity decreases with increasing ring size and molecular weight, in strong contrast to the behaviour of typical polymer melts (Fig. 18d). This surprising trend continues, up to a critical ring size, above which the viscosity increases with increasing molecular weight (ring size). It has been suggested that inter-ring correlations between catenated moieties may be a key cause for this behaviour. In fact, more complex catenated structures can even lead to a jamming transition as the ring size decreases.¹³⁶ Similarly, the dynamics of catenated rings were recently analysed in terms of a “topological friction,” which couples the motion of the interlocked portions of the molecules.¹³⁷ These findings suggest a rich phenomenology and motivate further synthetic and experimental advances so that these predictions can be tested and studied in the laboratory as well as the computer.

Conclusions and Outlook

In this review, the goal was to give an overview of the polycatenane field, from synthesis through theoretical studies. Certainly, such polymers grab the attention on account of their aesthetical appeal, but the growing polycatenane literature is showing how the mechanical bonds from catenated moieties

can result in new material properties. In all six classes of polycatenanes (Figure 1b-g) discussed, progress has been made. Templated catenane moieties and polymerization strategies can now be exploited to readily produce a wide range of polycatenanes and continued development and advances in this area are critical. As such, while early works focused on the polymerization of a preformed [2]catenane to yield poly[2]catenanes, work beyond these architectures, e.g., poly[*n*]catenanes and catenated networks, have started to gain traction. In addition, developments in spectroscopic, microscopic, material characterization and computational techniques have concurrently aided the understanding of these unique mechanically interlocked polymers.

While much progress has been made and there is an initial understanding of the impact of the catenane mechanical bond on the behaviour of a polymer, this review also highlights how much remains unknown. Correspondingly, understanding of the material properties of polycatenane polymers lags substantially behind that of other interlocked polymers, such as polyrotaxanes, slide ring gels and even more exotic interlocked macromolecules such as daisy chains, where synthetic routes are more developed and have allowed access to these MIPs on a large scale.

A significant challenge remains in the synthesis of most polycatenane structures, especially when it comes to accessing high molecular weight polymers with controlled ring sizes. To this end, an advance in synthetic methodologies will be required to access polycatenanes in higher yields and at scale. The clear challenge in this area remains the selectivity of catenation (ring closing) to linear by products. Solving this fundamental problem is needed to extend the interest of polycatenanes beyond the realm of synthetic chemists and into the hands of material scientists and engineers. Unfortunately, polycatenanes will continue to be the underrepresented sibling of the interlocked community as long as their synthesis, rather than the properties imparted by the interlocked structure, is the primary research focus. Of course, synthesis is a critical step but synthetic methodologies need to be developed that have the potential to be scalable and allow access to significant amounts of the interlocked polymer. Advances in computation and modelling of the catenanes is certainly providing critical insights to the properties of these materials, but development here too is required if we are going to understand the role of the mechanical bond in such complex structures, especially at longer time scales.

A lot of the work discussed here, beyond the synthesis, has focused on physical and mechanical properties of polycatenanes and this will certainly be a key avenue of polycatenane research for years to come. However, it is also worthwhile considering potential new functional or adaptive properties that the different polycatenane architectures may offer, especially as many moieties used to template their synthesis are inherently stimuli-responsive or redox-active. It can certainly be expected that an expanded library of polycatenanes will deepen the fundamental understanding of these unusual polymers and achieve new generations of

polymers with enhanced properties and diverse applications in the future.

Author Contributions

All authors contributed equally.

Conflicts of interest

There are no conflicts to declare

Acknowledgements

This work was funded by the National Science Foundation (NSF) grant number CHE-1903603. P.M.R. thanks the NSF for the award of a Graduate Research Fellowship, Grant No. 1746045.

Notes and references

- L. Garcia-Rio, F. J. Otero-Espinar, A. Luzardo-Alvarez and J. Blanco-Mendez, *Curr. Top. Med. Chem.*, 2014, **14**, 478–493.
- M. Arunachalam and H. W. Gibson, *Prog. Polym. Sci.*, 2014, **39**, 1043–1073.
- K. Ito, *Chem. Pharm. Bull. (Tokyo)*, 2017, **65**, 326–329.
- S. F. M. Van Dongen, S. Cantekin, J. A. A. W. Elemans, A. E. Rowan and R. J. M. Nolte, *Chem. Soc. Rev.*, 2014, **43**, 99–122.
- J. Rotzler and M. Mayor, *Chem. Soc. Rev.*, 2013, **42**, 44–62.
- K. Ito, in *Polyrotaxane and Slide-Ring Materials*, 2016, pp. 44–77.
- L. F. Hart, J. E. Hertzog, P. M. Rauscher, B. W. Rawe, M. M. Tranquilli and S. J. Rowan, *Nat. Rev. Mater.*, 2021, **6**, 508–530.
- N. H. Evans and P. D. Beer, *Chem. Soc. Rev.*, 2014, **43**, 4658.
- Z. Niu and H. W. Gibson, *Chem. Rev.*, 2009, **109**, 6024–6046.
- T. Takata, N. Kihara and Y. Furusho, *Adv. Polym. Sci.*, 2004, **171**, 1–75.
- H. Y. Au-Yeung, C. C. Yee, A. W. Hung Ng and K. Hu, *Inorg. Chem.*, 2018, **57**, 3475–3485.
- J.-L. Weidmann, D. Muscat, S. Mullins, C. Rosenauer, K. Martin, J.-M. Kern, J.-P. Sauvage, Y. Geerts, H. J. Räder and W. Köhler, *Chem. - A Eur. J.*, 2002, **5**, 1841–1851.
- Q. Wu, P. M. Rauscher, L. Xiaolong, R. J. Wojtecki, J. J. de Pablo, M. J. Hore and S. J. Rowan, *Science (80-)*, 2017, **358**, 1434–1439.
- F. Diederich, P. J. Stang and R. R. Tykwinski, Eds., *Modern Supramolecular Chemistry*, Wiley, 2008.
- Y. Geerts, D. Muscat and K. Müllen, *Macromol. Chem. Phys.*, 1995, **196**, 3425–3435.
- M. A. Olson, A. B. Braunschweig, L. Fang, T. Ikeda, R. Klajn, A. Trabolsi, P. J. Wesson, D. Benítez, C. A. Mirkin, B. A. Grzybowski and J. F. Stoddart, *Angew. Chemie Int. Ed.*, 2009, **48**, 1792–1797.
- J. Wang and A. L. Ferguson, *Macromolecules*, 2018, **51**, 598–616.
- D. Sun and J. Cho, *Phys. Rev. E*, 2014, **90**, 062601.
- M. Okada and A. Harada, *Macromolecules*, 2003, **36**, 9701–9703.
- T. Higashi, K. Morita, X. Song, J. Zhu, A. Tamura, N. Yui, K. Motoyama, H. Arima and J. Li, *Commun. Chem.*, 2019, **2**, 78.
- A. Li, Z. Tan, Y. Hu, Z. Lu, J. Yuan, X. Li, J. Xie, J. Zhang and K. Zhu, *J. Am. Chem. Soc.*, 2022, **144**, 2085–2089.
- M. B. Pinson, E. M. Sevick and D. R. M. Williams, *Macromolecules*, 2013, **46**, 4191–4197.
- K. Mayumi and K. Ito, *Polymer (Guildf)*, 2010, **51**, 959–967.
- E. Wasserman, *J. Am. Chem. Soc.*, 1960, **82**, 4433–4434.
- T. J. Hubin and D. H. Busch, *Coord. Chem. Rev.*, 2000, **200–202**, 5–52.
- J. E. M. Lewis, P. D. Beer, S. J. Loeb and S. M. Goldup, *Chem. Soc. Rev.*, 2017, **46**, 2577–2591.
- J. E. Beves, B. A. Blight, C. J. Campbell, D. A. Leigh and R. T. McBurney, *Angew. Chemie - Int. Ed.*, 2011, **50**, 9260–9327.
- L. Emmett, G. M. Prentice and G. D. Pantoş, *Annu. Reports Sect. 'B' (Organic Chem.)*, 2013, **109**, 217.
- D. G. Hamilton, J. K. M. Sanders, J. E. Davies, W. Clegg and S. J. Teat, *Chem. Commun.*, 1997, 897–898.
- J. F. Stoddart, *Angew. Chemie Int. Ed.*, 2017, **56**, 11094–11125.
- N. H. Evans, *European J. Org. Chem.*, 2019, **2019**, 3320–3343.
- C. O. Dietrich-Buchecker, J. P. Sauvage and J. P. Kintzinger, *Tetrahedron Lett.*, 1983, **24**, 5095–5098.
- L. Hogg, D. A. Leigh, P. J. Lusby, A. Morelli, S. Parsons and J. K. Y. Wong, *Angew. Chemie Int. Ed.*, 2004, **43**, 1218–1221.
- S. M. Goldup, D. A. Leigh, P. J. Lusby, R. T. McBurney and A. M. Z. Slawin, *Angew. Chemie*, 2008, **120**, 7107–7111.
- A.-M. L. Fuller, D. A. Leigh, P. J. Lusby, A. M. Z. Slawin and D. B. Walker, *J. Am. Chem. Soc.*, 2005, **127**, 12612–12619.
- G. Gil-Ramirez, D. A. Leigh and A. J. Stephens, *Angew. Chem., Int. Ed.*, 2015, **54**, 6110–6150.
- P. R. Ashton, T. T. Goodnow, A. E. Kaifer, M. V. Reddington, A. M. Z. Slawin, N. Spencer, J. F. Stoddart, C. Vicent and D. J. Williams, *Angew. Chemie Int. Ed. English*, 1989, **28**, 1396–1399.
- W. R. Dichtel, O. Š. Miljanić, W. Zhang, J. M. Spruell, K. Patel, I. Aprahamian, J. R. Heath and J. F. Stoddart, *Acc. Chem. Res.*, 2008, **41**, 1750–1761.
- M. A. Olson, A. Coskun, L. Fang, A. N. Basuray and J. F. Stoddart, *Angew. Chemie Int. Ed.*, 2010, **49**, 3151–3156.
- C. A. Hunter and D. H. Purvis, *J. Am. Chem. Soc.*, 1992, **114**, 5303–5311.
- F. Vögtle, S. Meier and R. Hoss, *Angew. Chemie Int. Ed. English*, 1992, **31**, 1619–1622.
- H. Iwamoto, W. Takizawa, K. Itoh, T. Hagiwara, E. Tayama, E. Hasegawa and T. Haino, *J. Org. Chem.*, 2013, **78**, 5205–5217.
- E. N. Guidry, S. J. Cantrill, J. F. Stoddart and R. H. Grubbs, *Org. Lett.*, 2005, **7**, 2129–2132.
- T. J. Kidd, D. A. Leigh and A. J. Wilson, *J. Am. Chem. Soc.*, 1999, **121**, 1599–1600.
- M. Prakashni, R. Shukla and S. Dasgupta, *J. Org. Chem.*,

- 2021, **86**, 7825–7831.
- 46 C. N. Marrs and N. H. Evans, *Org. Biomol. Chem.*, 2015, **13**, 11021–11025.
- 47 H. Iwamoto, S. Tafuku, Y. Sato, W. Takizawa, W. Katagiri, E. Tayama, E. Hasegawa, Y. Fukazawa and T. Haino, *Chem. Commun.*, 2016, **52**, 319–322.
- 48 D. Muscat, A. Witte, W. Köhler, K. Müllen and Y. Geerts, *Macromol. Rapid Commun.*, 1997, **18**, 233–241.
- 49 D. Muscat, W. Köhler, H. J. Räder, K. Martin, S. Mullins, B. Müller, K. Müllen and Y. Geerts, *Macromolecules*, 1999, **32**, 1737–1745.
- 50 C.-A. Fustin, C. Bailly, G. J. Clarkson, P. De Groote, T. H. Galow, D. A. Leigh, D. Robertson, A. M. Z. Slawin and J. K. Y. Wong, *J. Am. Chem. Soc.*, 2003, **125**, 2200–2207.
- 51 C.-A. Fustin, G. J. Clarkson, D. A. Leigh, F. Van Hoof, A. M. Jonas and C. Bailly, *Macromolecules*, 2004, **37**, 7884–7892.
- 52 A. Van Quaethem, P. Lussis, D. A. Leigh, A.-S. Duwez and C.-A. Fustin, *Chem. Sci.*, 2014, **5**, 1449–1452.
- 53 C.-A. Fustin, C. Bailly, G. J. Clarkson, T. H. Galow and D. A. Leigh, *Macromolecules*, 2004, **37**, 66–70.
- 54 H. Xing, Z. Li, Z. L. Wu and F. Huang, *Macromol. Rapid Commun.*, 2018, **39**, 1700361.
- 55 B. N. Ahamed, P. Van Velthem, K. Robeyns and C.-A. Fustin, *ACS Macro Lett.*, 2017, **6**, 468–472.
- 56 H. Xing, Z. Li, W. Wang, P. Liu, J. Liu, Y. Song, Z. L. Wu, W. Zhang and F. Huang, *CCS Chem.*, 2020, **2**, 513–523.
- 57 W. Wang and H. Xing, *Polym. Chem.*, 2018, **9**, 2087–2091.
- 58 C. Hamers, F. M. Raymo and J. F. Stoddart, *European J. Org. Chem.*, 1998, **1998**, 2109–2117.
- 59 D. L. Simone and T. M. Swager, *J. Am. Chem. Soc.*, 2000, **122**, 9300–9301.
- 60 M. Bria, J. Bigot, G. Cooke, J. Lyskawa, G. Rabani, V. M. Rotello and P. Woisel, *Tetrahedron*, 2009, **65**, 400–407.
- 61 Y. Gan, D. Dong and T. E. Hogen-Esch, *Macromolecules*, 2002, **35**, 6799–6803.
- 62 P.-F. Cao, J. D. Mangadlao, A. de Leon, Z. Su and R. C. Advincula, *Macromolecules*, 2015, **48**, 3825–3833.
- 63 A. Bunha, M. C. Tria and R. Advincula, *Chem. Commun.*, 2011, **47**, 9173–9175.
- 64 A. K. Bunha, J. Mangadlao, M. J. Felipe, K. Pangilinan and R. Advincula, *Macromol. Rapid Commun.*, 2012, **33**, 1214–1219.
- 65 A. Bunha, P.-F. Cao, J. Mangadlao, F.-M. Shi, E. Foster, K. Pangilinan and R. Advincula, *Chem. Commun.*, 2015, **51**, 7528–7531.
- 66 K. Ishikawa, T. Yamamoto, M. Asakawa and Y. Tezuka, *Macromolecules*, 2010, **43**, 168–176.
- 67 Y. Ohta, M. Nakamura, Y. Matsushita and A. Takano, *Polymer (Guildf.)*, 2012, **53**, 466–470.
- 68 K. Morita, K. Motoyama, A. Kuramoto, R. Onodera and T. Higashi, *J. Incl. Phenom. Macrocycl. Chem.*, 2021, **100**, 169–175.
- 69 D. B. Amabilino, P. R. Ashton, A. S. Reder, N. Spencer and J. F. Stoddart, *Angew. Chemie Int. Ed. English*, 1994, **33**, 1286–1290.
- 70 D. B. Amabilino, P. R. Ashton, S. E. Boyd, J. Y. Lee, S. Menzer, J. F. Stoddart and D. J. Williams, *Angew. Chemie Int. Ed. English*, 1997, **36**, 2070–2072.
- 71 N. Watanabe, Y. Ikari, N. Kihara and T. Takata, *Macromolecules*, 2004, **37**, 6663–6666.
- 72 M. M. Tranquilli, Q. Wu and S. J. Rowan, *Chem. Sci.*, 2021, **12**, 8722–8730.
- 73 S. Datta, Y. Kato, S. Higashiharaguchi, K. Aratsu, A. Isobe, T. Saito, D. D. Prabhu, Y. Kitamoto, M. J. Hollamby, A. J. Smith, R. Dalgliesh, N. Mahmoudi, L. Pesce, C. Perego, G. M. Pavan and S. Yagai, *Nature*, 2020, **583**, 400–405.
- 74 P.-G. de Gennes, *Scaling concepts in polymer physics*, Cornell University Press, Ithaca, 1979.
- 75 E. Raphaël, C. Gay and P.-G. de Gennes, *J. Stat. Phys.*, 1997, **89**, 111–118.
- 76 G. T. Pickett, *Eur. Lett.*, 2006, **76**, 616–622.
- 77 J. Fischer, M. Lang and J.-U. Sommer, *J. Chem. Phys.*, 2015, **143**, 243114.
- 78 R. Arakawa, T. Watanabe, T. Fukuo and K. Endo, *J. Polym. Sci. Part A Polym. Chem.*, 2000, **38**, 4403–4406.
- 79 K. Endo, T. Shiroi, N. Murata, G. Kojima and T. Yamanaka, *Macromolecules*, 2004, **37**, 3143–3150.
- 80 H. Ishida, A. Kisanuki and K. Endo, *Polym. J.*, 2009, **41**, 110.
- 81 K. Endo and T. Yamanaka, *Macromolecules*, 2006, **39**, 4038–4043.
- 82 R. Takashima, D. Aoki and H. Otsuka, *Macromolecules*, 2021, **54**, 8154–8163.
- 83 P. Hu, J. Madsen, Q. Huang and A. L. Skov, *ACS Macro Lett.*, 2020, **9**, 1458–1463.
- 84 G. Riou and E. Delain, *Proc. Natl. Acad. Sci.*, 1969, **62**, 210–217.
- 85 D. P. Cavalcanti, D. L. Gonçalves, L. T. Costa and W. de Souza, *Micron*, 2011, **42**, 553–559.
- 86 P. Borst and J. H. J. Hoeijmakers, *Plasmid*, 1979, **2**, 20–40.
- 87 H. C. Renger and D. R. Wolstenholme, *J. Cell Biol.*, 1972, **54**, 346–364.
- 88 M. A. Krasnow and N. R. Cozzarelli, *J. Biol. Chem.*, 1982, **257**, 2687–2693.
- 89 W. Waldeck, M. Theobald and H. Zentgraf, *EMBO J.*, 1983, **2**, 1255–1261.
- 90 Y. S. Kim, B. Kundukad, A. Allahverdi, L. Nordensköld, P. S. Doyle and J. R. C. van der Maarel, *Soft Matter*, 2013, **9**, 1656–1663.
- 91 B. A. Krajina, A. Zhu, S. C. Heilshorn and A. J. Spakowitz, *Phys. Rev. Lett.*, 2018, **121**, 148001.
- 92 A. R. Klotz, B. W. Soh and P. S. Doyle, *Proc. Natl. Acad. Sci. U. S. A.*, 2020, **117**, 121–127.
- 93 A. Vologodskii and V. V. Rybenkov, *Phys. Chem. Chem. Phys.*, 2009, **11**, 10543–10552.
- 94 M. Bohn and D. W. Heermann, *J. Chem. Phys.*, 2010, **132**, 044904.
- 95 M. Rubinstein and R. H. Colby, *Polymer Physics*, Oxford University Press, New York, 2003.
- 96 S. F. Edwards, *Proc. Phys. Soc.*, 1967, **91**, 513–519.
- 97 S. F. Edwards, *J. Phys. A Gen. Phys.*, 1968, **1**, 15–28.
- 98 K. Iwata, *J. Chem. Phys.*, 1982, **76**, 6363–6374.
- 99 K. Iwata and T. Kimura, *J. Chem. Phys.*, 1981, **74**, 2039–2048.
- 100 G. Marrucci, *Macromolecules*, 1981, **14**, 434–442.

- 101 K. Iwata, *J. Chem. Phys.*, 1983, **78**, 2778–2787.
- 102 K. Iwata and S. F. Edwards, *J. Chem. Phys.*, 1989, **90**, 4567–4581.
- 103 F. Tanaka, *Prog. Theor. Phys.*, 1982, **68**, 148–163.
- 104 F. Tanaka, *Prog. Theor. Phys.*, 1982, **68**, 164–177.
- 105 F. Tanaka, *J. Chem. Phys.*, 1987, **87**, 4201–4206.
- 106 R. C. Ball, M. Doi, S. F. Edwards and M. Warner, *Polymer (Guildf.)*, 1981, **22**, 1010–1018.
- 107 S. F. Edwards and T. Vilgis, *Polymer (Guildf.)*, 1986, **27**, 483–492.
- 108 W. W. Graessley and D. S. Pearson, *J. Chem. Phys.*, 1977, **66**, 3363–3370.
- 109 M. Otto, *J. Phys. A. Math. Gen.*, 2001, **34**, 2539–2547.
- 110 M. G. Brereton, *J. Phys. A. Math. Gen.*, 2001, **34**, 5131.
- 111 T. C. B. McLeish, *Adv. Phys.*, 2002, **51**, 1379–1527.
- 112 M. D. Frank-Kamenetskii, A. V. Lukashin and A. V. Vologodskii, *Nature*, 1975, **258**, 398–402.
- 113 P. M. Rauscher, S. J. Rowan and J. J. De Pablo, *ACS Macro Lett.*, 2018, **7**, 938–943.
- 114 Z. Ahmadian Dehaghani, I. Chubak, C. N. Likos and M. R. Ejtehadi, *Soft Matter*, 2020, **16**, 3029–3038.
- 115 M. Bohn, D. W. Heermann, O. Lourenço and C. Cordeiro, *Macromolecules*, 2010, **43**, 2564–2573.
- 116 P. M. Rauscher, K. S. Schweizer, S. J. Rowan and J. J. De Pablo, *Macromolecules*, 2020, **53**, 3390–3408.
- 117 J. Li, F. Gu, N. Yao, H. Wang and Q. Liao, *ACS Macro Lett.*, 2021, **10**, 1094–1098.
- 118 A. Marantan and L. Mahadevan, *Am. J. Phys.*, 2018, **86**, 86–94.
- 119 S. M. Mirkin, in *DNA Topology: Fundamentals. in eLS*, (Ed.), John Wiley & Sons, Ltd, Chichester, UK, 2001.
- 120 K. N. Kreuzer and N. R. Cozzarelli, *Cell*, 1980, **20**, 245–254.
- 121 M. Otto, *J. Phys. A. Math. Gen.*, 2004, **37**, 2881–2893.
- 122 F. Ferrari, *Ann. Phys.*, 2002, **11**, 255–290.
- 123 M. Otto and T. A. Vilgis, *Phys. Rev. Lett.*, 1998, **80**, 881–884.
- 124 M. Caraglio, C. Micheletti and E. Orlandini, *Polymers (Basel.)*, 2017, **9**, 327.
- 125 T. A. Vilgis and M. Otto, *Phys. Rev. E*, 1997, **56**, R1314–R1317.
- 126 M. Lang, J. Fischer, M. Werner and J.-U. Sommer, *Macromol. Symp.*, 2015, **358**, 140–147.
- 127 M. Lang, J. Fischer, M. Werner and J. U. Sommer, *Phys. Rev. Lett.*, 2014, **112**, 238001.
- 128 D. Michieletto, D. Marenduzzo and E. Orlandini, *Phys. Biol.*, 2015, **12**, 036001.
- 129 J. M. Polson, E. J. Garcia and A. R. Klotz, *Soft Matter*, 2021, **17**, 10505–10515.
- 130 B. W. Soh and P. S. Doyle, *ACS Macro Lett.*, 2020, **9**, 944–949.
- 131 B. W. Soh and P. S. Doyle, *ACS Macro Lett.*, 2021, **10**, 880–885.
- 132 I. Yadav, D. Al Sulaiman, B. W. Soh and P. S. Doyle, *ACS Macro Lett.*, 2021, **10**, 1429–1435.
- 133 P. M. Rauscher, S. J. Rowan and J. J. De Pablo, *Phys. Rev. E*, 2020, **102**, 032502.
- 134 H. Lei, J. Zhang, L. Wang and G. Zhang, *Polymer (Guildf.)*, 2021, **212**, 123160.
- 135 P. M. Rauscher, K. S. Schweizer, S. J. Rowan and J. J. de Pablo, *J. Chem. Phys.*, 2020, **152**, 214901.
- 136 K. Hagita, T. Murashima and N. Sakata, *Macromolecules*, 2021, **55**, 166–177.
- 137 G. Amici, M. Caraglio, E. Orlandini and C. Micheletti, *ACS Macro Lett.*, 2021, **13**, 1–6.



Guancen Liu studied Chemistry at the University of Florida, working on supramolecular assembly of paracyclophanes under the supervision of Prof. Ronald K. Castellano. He received his B.S. in Chemistry and graduated Summa Cum Laude in 2020. In 2021, he joined Prof. Stuart J. Rowan's group in the department of Chemistry at the University of Chicago. He is devoted to the development of new poly[n]catenanes and other interlocked macromolecules for their unique chemical and material properties.



Marissa M. Tranquilli received her B.A. degrees in both Chemistry and English Literature from Cornell University in 2015. In 2016 she began her graduate work in the Department of Chemistry at the University of Chicago, working under Prof. Stuart J. Rowan. She received her M.S. in 2017 and is currently continuing her research into the understanding and development of new poly[n]catenane compounds in pursuit of her doctoral degree.



Phillip M. Rauscher is a Research Scientist at Solvay Materials. He obtained his B.S. in Physics and Chemistry in 2013 from Emory University, conducting research under the supervision of Prof. Connie B. Roth. In 2016, he joined the Pritzker School of Molecular Engineering at the University of Chicago as a graduate student co-advised by Profs. Juan J. de Pablo and Stuart J. Rowan. Upon completing his Ph.D. in 2020, he transitioned to a postdoctoral role in the de Pablo group until 2021, when he joined the Polymer Physics group at Solvay Materials. His research focuses on molecular simulations of soft matter systems, with emphasis on topology, rheology and mechanics of polymers, interfacial transport, glassy materials, and nonequilibrium thermodynamics.



Stuart J. Rowan is the Barry L. MacLean Professor of Molecular Engineering at the University of Chicago. He grew up in Scotland and received his B.Sc. (1991) and PhD (1995) from the University of Glasgow. He carried out postdoctoral research with Jeremy K. M. Sanders (Cambridge) and Sir J. Fraser Stoddart (UCLA) before starting his independent career at Case Western Reserve University (1999). In 2016 he moved to the University of Chicago. He is an ACS Fellow, a Fellow of the Royal Society of Chemistry and the Editor-in-Chief of ACS Macro Letters.



Benjamin Rawe was born in 1989 in Burton upon Trent, England. In 2011 he received his MSci (Honours) from the University of Bristol completing a research thesis on scorpionate complexes with Gareth R. Owen. In 2011 he joined the chemistry department at the University of British Columbia, Vancouver to pursue his Ph.D. under the supervision of Derek P. Gates on phosphorus containing macromolecules. Upon completion of his Ph.D. he transitioned to a postdoctoral role in the Gates lab until 2018 when he joined the Rowan group at the University of Chicago as a postdoctoral scholar. His research in the Rowan lab focuses on developing synthetic methods to high molecular weight poly[n]catenanes. A secondary interest is establishing structure property relationships for recyclable polyolefin materials.